Journal of Hydrology 598 (2021) 125735

Contents lists available at ScienceDirect

Journal of Hydrology

journal homepage: www.elsevier.com/locate/jhydrol

Research papers

Assessment of the cascade of uncertainty in future snow depth projections across watersheds of mountainous, foothill, and plain areas in northern latitudes

Majid Zaremehrjardy [a], Saman Razavi [b], Monireh Faramarzi [a,*]

[a] Watershed Science & Modeling Laboratory, Department of Earth and Atmospheric Sciences, University of Alberta, Edmonton, AB T6G 2R3, Canada

[b] Global Institute for Water Security, School of Envionment and Sustainability, and Department of Civil, Geological, and Environmental Enigeering, University of Saskatchewan, Canada

ARTICLE INFO

This manuscript was handled by Emmanouil Anagnostou, Editor-in-Chief

Keywords:
Regional hydrology
Uncertainty decomposition
Snowmelt projection
Energy Balance
Temperature Index
SWAT

ABSTRACT

Snowmelt is a major driver of the hydrological cycle in cold regions, as such, its accurate representation in hydrological models is key to both regional snow depth and streamflow prediction. The choice of a proper method for snowmelt representation is often improvised; however, a thorough characterization of uncertainty in such process representations particularly in the context of climate change has remained essential. To fill this gap, this study revisits and characterizes performance and uncertainty around the two general approaches to snowmelt representation, namely Energy-Balance Modules (EBMs) and Temperature-Index Modules (TIMs). To account for snow depth simulation and projection, two common Snow Density formulations (SNDs) are implemented that map snow water equivalent (SWE) to snow depth. The major research questions we address are two-fold. First, we examine the dominant controls of uncertainty in snow depth and streamflow simulations across scales and in different climates. Second, we evaluate the cascade of uncertainty of snow depth projections resulting from impact model parameters, greenhouse gas emission scenarios, climate models and their internal variability, and downscaling processes. We enable the Soil and Water Assessment Tool (SWAT) by coupling EBM, TIM, and two SND modules for examination of different snowmelt representation methods, and Analysis of Variance (ANOVA) for uncertainty decomposition and attribution. These analyses are implemented in mountainous, foothill, and plain regions in a large snow-dominated watershed in western Canada. Results show, rather counter-intuitively, that the choice of SND is a major control of performance and uncertainty of snow depth simulation rather than the choice between TIMs and EBMs and of their uncertain parameters. Also, analysis of streamflow simulations suggest that EBMs generally overestimate streamflow on main tributaries. Finally, uncertainty decompositions show that parameter uncertainty related to snowmelt modules dominantly controls uncertainty in future snow depth projections under climate change, particularly in mountainous regions. However, in plain regions, the uncertainty contribution of model parameters becomes more variable with time and less dominant compared with the other sources of uncertainty. Overall, it is shown that the hydro-climatic and topographic conditions of different regions, as well as input data availability, have considerable effect on reproduction of snow depth, snowmelt and resulting streamflow, and on the share of different uncertainty sources when projecting regional snow depth.

1. Introduction

Snowmelt is one of the most important components of the hydrological cycle, as it controls the magnitude and dynamics of snow depth, streamflow, and flood frequency, especially in mountainous regions with high climate variability (Zeinivand and de Smedt, 2010; Abbas et al., 2019). Snowmelt is dependent on various climatological and geophysical factors including, but not limited to, precipitation, temperature, solar radiation and vegetation cover. The dynamics and properties of such factors are expected to change in time and space under future climate conditions; hence, the impact of climate change on snowmelt dynamics can be substantial (Raleigh and Clark, 2014;

* Corresponding author.
E-mail address: faramarz@ualberta.ca (M. Faramarzi).

https://doi.org/10.1016/j.jhydrol.2020.125735
Received 3 June 2020; Received in revised form 26 October 2020; Accepted 2 November 2020
Available online 18 November 2020

Verdhen et al., 2014a). Therefore, it is essential to understand the governing factors and processes that control snowmelt and how they might change over time under current and future conditions. An improved understanding can enable hydrologists and water managers to reduce uncertainty for future planning and management of water resources, and adaptation to climate change (Pradhanang et al., 2011).

Recently, process-based hydrological models have been used to simulate snow accumulation and snowmelt in different regions with various levels of areal extent and climate conditions. These models include, but are not limited to, Cold Regions Hydrological Model (CRHM) (DeBeer and Pomeroy, 2017; Fang et al., 2010), Variable Infiltration Capacity (VIC) (Barnhart et al., 2016; Islam et al., 2017) and Soil and Water Assessment Tool (SWAT) (Pradhanang et al., 2011; Qi et al., 2017; Tiwari et al., 2018). In hydrological models, snowmelt simulation is carried out through two widely-used approaches, namely Temperature-Index Modules (TIMs) and Energy-Balance Modules (EBMs) (Debele et al., 2010). TIMs (also known as degree-day methods) are generally regarded as a simple and parsimonious approach for snowmelt estimation, as they are solely dependent on air temperature and snowpack (Hock, 2003; Debele et al., 2010). EBMs, however, are more complex and parameterized, as they try to comprehensively account for energy exchanges in air-and-snowpack and snowpack-and-soil interfaces (Dingman, 2015). While comparative assessments of TIMs and EBMs in snowmelt simulation models have widely been studied across different regions, the choice of the best model for hydrologic modelling in particular at regional scales remains a controversy (Zhang et al., 2008; Pradhanang et al., 2011).

EBMs are generally expected to outperform TIMs in simulating snowmelt dynamics, mainly because of their more realistic and physically-based nature (Todd Walter et al., 2005; Fuka et al., 2012; Qi et al., 2017; Massmann, 2019). Nevertheless, several studies have suggested that TIMs may perform equally well or even better than EBMs do in the representation of snowmelt and snow depth dynamics (e.g., Franz et al., 2008; Debele et al., 2010; Verdhen et al., 2014a). In addition, a disadvantage of EBMs is that they are more data-intensive and demand numerous forcing inputs, many of which cannot be directly measured or quantified at scales larger than an instrumented site (Bavera et al., 2014; Raleigh et al., 2016; Mas et al., 2018). The issues around data demands are exacerbated in regional studies with climate and land cover heterogeneity, especially in mountainous regions where regionalized data of energy-based variables such as snow albedo, snow surface temperature, emissivity and temperature lapse rate are difficult and costly to measure (Najafi et al., 2017; Raleigh et al., 2016; Sun et al., 2019). Furthermore, the adequacy of any of TIMs and EBMs depends on the properties of driving climate forces in the region of interest. For instance, while use of EBMs in maritime regions with more rain-on-snow events has proven more suitable, TIMs can be considered better options in regions where net solar radiation, which is a proxy for air temperature, is the dominant heat source (Debele et al., 2010; Qi et al., 2017). Consequently, the heterogeneity in climate, land cover, and topography across large river basins results in the dominancy of different snowmelt mechanisms in different parts. Most of previous studies, however, have investigated and compared the adequacy of TIMs or EBMs in small-scale areas where extensive data is available (e.g., Franz et al., 2008; Tobin et al., 2013; Aggarwal et al., 2014; Fu et al., 2015); some other studies focused on larger but relatively homogeneous areas in terms of land cover, climate, and topography (for instance, Ficklin and Barnhart, 2014; Troin et al., 2015a; Haghnegahdar et al., 2017). Hence, the performance of TIMs and EBMs in snowmelt simulation in regional studies with high variability of topography, climate, and land-use is yet to be properly understood.

The availability of extensive and reliable data is key to successful model parametrization and simulation of snowmelt and snow depth in regional hydrological models (Shrestha et al., 2012; Mas et al., 2018). At field scales where sufficient field data is available, high-fidelity snowmelt models can be developed (e.g., Pomeroy et al., 1998; Harder et al., 2018). At larger scales, however, where field data coverage is limited, some physical characteristics of the basin need to be represented in models by user-defined 'effective' parameters (Mas et al., 2018). Identifying such parameters that control the representation of physical processes in regional hydrological models is critical for short-term predictions and also projections of how the basin future might look like under climate change (Singh and Frevert, 2002). Parameter identification in snowmelt and streamflow projections is mostly done through optimization-based approach (Razavi et al., 2010), where the best set of parameter values according to some goodness-of-fit criteria is identified and used for prediction and scenario runs (e.g., Franz et al., 2008; Zeinivand and de Smedt, 2010; Pradhanang et al., 2011; Qi et al., 2017; Liu et al., 2018). However, it is well-known that the proper parameter values are typically *non-unique* in any given problem, a phenomenon that is commonly referred to as equifinality (Beven and Freer, 2001; Fu et al., 2015). To address equifinality, uncertainty-based approaches are used, where several well-performing sets of parameter values form optimal ranges for parameters to account for input data, model structure, and parameter uncertainty (e.g., Faramarzi et al., 2009, 2017; Renard et al., 2010; Wu et al., 2017; Ahmadalipour et al., 2018).

Model structure uncertainty (e.g., EBMs versus TIMs) and parameter uncertainty within hydrological modelling are two of the many uncertainty sources in the 'cascade of uncertainty' for climate change impact assessment. Other sources include Global and Regional Climate Models (GCMs and RCMs), Representative Concentration Pathways (RCPs), and downscaling methods (Chen et al., 2011b; Bosshard et al., 2013). When dealing with the cascade of uncertainty in climate change impact assessments, it is important to decompose and apportion the predictive uncertainty to the different uncertainty sources. The Analysis of Variance (ANOVA) has frequently been used for this purpose (e.g., Déqué et al., 2007; Yip et al., 2011; Bosshard et al., 2013). ANOVA is the basis of the well-established variance-based approach to global sensitivity analysis (GSA) for uncertainty apportionment (Razavi and Gupta, 2019; Sobol', 1993). We note that ANOVA, and GSA in general, is not a means to quantify uncertainty in different sources; instead, it breaks down the total uncertainty in the output and attributes its pieces to different uncertainty sources and their interactions. This way, ANOVA identifies the dominant controls of predictive uncertainty, and also the factors whose uncertainty does not matter much. Furthermore, ANOVA is suitable for this study because there is no correlation structure between the uncertainty sources that are under investigation here as they are fundamentally different – refer to Do and Razavi (2020) for a discussion on this issue.

The majority of studies for apportionment of uncertainty in future projections addressed only uncertainty from climate models, emission scenarios, and downscaling techniques (Kim et al., 2019). Recent studies quantified the uncertainty contribution from hydrological model parameters and input data to the uncertainty in projection of future streamflow (Jung et al., 2012; Prudhomme and Davies, 2009; Vetter et al., 2017; Wilby and Harris, 2006), green water and blue water flows (Ashraf Vaghefi et al., 2019), and Snow Water Equivalent (SWE) (Poulin et al., 2011). In this regard, the uncertainty due to the choice of TIMs and EBMs along with their parameterizations and its impact on uncertainty in snowmelt and snow depth projections under a changing climate has not been quantified. Unlike TIMs, EBMs are more physically-based and therefore they demand more extensive spatiotemporal data to run. As such high resolution data may not be available at regional scales, calibration parameters are needed to be assigned to unknown input variables required by EBMs. Therefore, it is essential to quantify the effects of TIMs (as simpler, less parametrized modules) and EBMs (as more complex, more parameterized modules) on snow depth projections under climate change scenarios in large watersheds with diverse hydrologic, climatic, and geospatial conditions.

Another major but often ignored research gap in hydrologic modelling of cold regions is the representation of snowpack in those models, which is in the form of SWE (Avanzi et al., 2015) and is directly calculated from snowmelt modules. However, measurements of snow that are used for model evaluation are often available only as snow depths, not SWE (Sturm et al., 2010). Therefore, the accurate estimation of snow density (SND) that converts simulated SWE (i.e., in mm water) to snow depth (i.e., in mm snow depth) and vice versa becomes key to credible modelling of snow processes at regional scales. An accurate estimation of SWE, SND, and the conversion to snow depth is possible within field scales (Jost et al., 2007; Young et al., 2013; Li et al., 2017). However, field measurements in large regions are time-consuming, costly, and complicated because of heterogeneity in topography and natural conditions, and therefore, only a limited number of snow surveys can be available for a watershed (Bocchiola and Groppelli, 2010; Avanzi et al., 2015). As such, reliable estimation of SND in locations where it is not measured is essential. The variability and distribution of SND has been widely studied using empirical relationships, where the snow density is reproduced as a function of various variables such as air temperature, snow depth, SWE, among other predictors (e.g., Avanzi et al., 2015; Jonas et al., 2009; McCreight and Small, 2014; Mizukami and Perica, 2008). Most of such relations are acquired based on a particular area of study (Avanzi et al., 2015). Thus, it is essential to evaluate and compare the performance of various SND estimators, since a careful choice of SND equation is necessary for a reliable simulation of snow depth in a particular region (e.g., maritime regions vs. prairie regions).

The overarching goal of this study is to provide an improved understanding of uncertainty associated with simulation and projection of snow depth and snowmelt dynamics in regional hydrological modelling under current and future climate conditions. To this end, we enable Soil and Water Assessment Tool (SWAT) with both TIM and EBM snowmelt modules and two different SND parametrizations, by modifying its source code, to comprehensively assess the model structural and parametric uncertainty. We utilize ANOVA to apportion the total uncertainty in snow depth projections into uncertainty arising from not only hydrological model structure (i.e., TIMs and EBMs), parameters, and input data, but also the choice of climate models and their structures, greenhouse gas emission scenarios, and downscaling methods. The more specific objectives of this paper are threefold as it investigates: (1) the performance of EBM and TIMs, through examining spatiotemporal variability of snow depth and streamflow simulations in mountainous, foothill and plain areas by using a large snow-dominated watershed in Western Canada; (2) the spatiotemporal changes in cascade of uncertainty associated with snow depth projections using EBMs and TIMs as snowmelt modules in regional hydrological modelling under different climate change models, RCP scenarios, and downscaling methods; and (3) the effect of SND formulation on the simulations and projections of snow depth and its impact on the projected cascade of uncertainty.

2. Study area and data

2.1. Study area

North Saskatchewan River Basin (NSRB) is a large watershed with considerable variability in climate, topography, and land cover, located in the central area of Alberta, western Canada. The area of NSRB is 59,128 km^2, forming approximately 9% of landmass in the province of Alberta (North Saskatchewan Watershed Alliance, 2005). The NSRB originates from Columbia Icefields and the foothill regions of Rocky Mountains in the west of Alberta (Fig. 1a). The watershed is characterized by a diverse topography, with the elevation of NSRB ranging from 3478 MASL on the mountainous region down to less than 500 MASL on the plain areas towards east of Alberta (Fig. 1b). The land cover changes from high mountains and icefields (i.e., mountain glaciers) in the west, to evergreen forests in the foothills, and urban and agricultural areas as well as pastures are among other land cover classes in the majority of the plain region in the east of the watershed (Fig. 1a). The historical climate data of NSRB for 1983–2007 shows a temperature range from less than −30 °C in winters up to + 29 °C in summers for the watershed, and the average annual precipitation ranging from 760 mm year^{-1} in mountainous areas to 400 mm year^{-1} on the plain region. Snowfall and snow cover dominate the watershed for at least five months of the year (Government of Canada, 2019). This suggests a noticeable variance of climate, topography and land cover in time and space throughout the NSRB.

The NSRB is a major basin draining to the Saskatchewan River in Canadian Prairies that drains into the Hudson Bay and to Atlantic Ocean. An average value of 7000 million cubic meters of water is annually discharged from North Saskatchewan River (NSR) to the Saskatchewan River at the Alberta-Saskatchewan border on the east side of NSRB (Alberta Environment and Parks, 2019). The NSR also provides the drinking water for the urban areas within NSRB, including the city of Edmonton. Two hydro-electric dams named Bighorn and Brazeau Dams are located in the mountainous regions of NSRB, with an overall productivity of 800,000 MWh year^{-1} (MacDonald et al., 2012). Moreover, numerous small and large glaciers located in the Rocky Mountains are important contributors to the streamflow in the upstream tributaries of this river (Fig. 1a).

2.2. Historical climate and geospatial data

Historical climate data including daily precipitation, temperature, solar radiation, humidity, and wind speed were used from Faramarzi et al. (2015), who used a suit of four climate time series from local meteorological, gridded produscts, and satellite data at a provincial coverage to reproduce historical streamflow records by implementing a

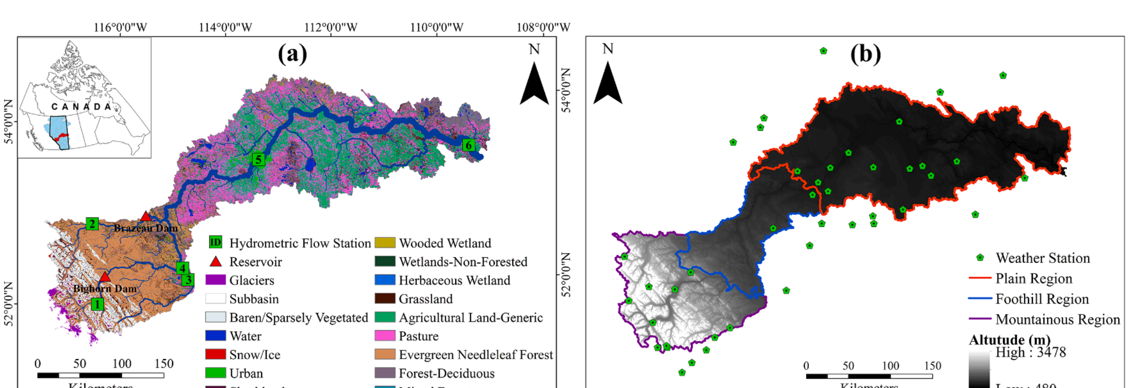

Fig. 1. Map of NSRB representing geographic distribution of (a) the main river basin, two main dams, hydrometric stations and land use-land cover classes; and (b) topographic range, weather stations, and the three hydrologic regions used for assessment of model results.

calibrated hydrologic model. Other data including vegetation cover, soil characteristics, operation of dams, and glacial maps and their daily time series were obtained from Faramarzi et al. (2017). In order to examine the effects of snowmelt simulation approaches (i.e., EBM and TIM) on streamflow dynamics in different regions of NSRB, six important hydrometric stations were considered for observing model performance and uncertainty analysis within different regions of this watershed. The locations and properties of these stations are shown in Fig. 1 and the details are provided in Table S2. Observed streamflow data for multiple hydrometric stations were collected from Environment and Climate Change Canada (Table S1). Finally, in order to assess the performance of snow depth simulations using the two EBM and TIM approaches, the simulated depth data were compared with the monthly gridded snow depth data acquired from Canadian Meteorological Centre (CMC) Daily Snow Depth Analysis Data, Version 1 (Brown and Bransnett, 2010). The monthly CMC snow depth data were available from January 1999 at a spatial resolution of 24 km × 24 km, and they were used to validate EBM and TIM simulations for 1999–2007 period.

2.3. Future climate projection data

To simulate future changes in the snow depth projections of NSRB, future climate projections from the Pacific Climate Impacts Consortium (PCIC) (Cannon, 2015) were used in this study. PCIC provides statistically downscaled GCM climate scenarios from 1950 to 2100 (Bürger et al., 2013) based on the Coupled Model Intercomparison Project phase 5 (CMIP5) (Taylor et al., 2012) and the historical daily gridded climate data from NRCANmet (ANUSPLINE) for Canada (McKenney et al., 2011). The choice of GCMs was based on climate models that resulted in the widest range of projected future climate for the Western North America region (Ammar et al., 2020; Cannon, 2015). On the other hand, the GCMs are forced with different Representative Concentration Pathways (RCPs), which define a specific emissions trajectory and subsequent radiative forcing in the earth-atmosphere system. Out of four pathways developed for the year of 2100, we chose RCP 2.6 and RCP 8.5 (representing very low and very high forcing levels, respectively) to account for the widest range of projected radiative forcing (van Vuuren et al., 2011). PCIC provides Canada-wide downscaled climate change projections using the Bias Correction/Constructed Analogues with Quantile mapping reordering (BCCAQ) method (http://www.pacificclimate.org/data).

To test the effect of downscaling procedures on the future projections of snow depth, we used two different downscaled products. The first one is the aforementioned downscaled data from PCIC (named DS1 in Fig. 2). The second product is a set of further downscaled PCIC data to Alberta condition (named DS2, Fig. 2) based on daily historical climate data from earlier studies by Ammar et al. (2020) and Masud et al. (2018). In their study, historical climate data is from a study by Faramarzi et al. (2015), where a suite of four climate data sources including meteorological station-based and gridded products were examined to reproduce historical flow records for 130 gauging stations in Alberta by using a physically process-based hydrological model. A "combination" approach, where several climate data were combined from different sources, was found to be best in generating their corresponding streamflow. This historical climate dataset was later used in Ammar et al. (2020) and Masud et al. (2018) studies for a second-order bias-correction of the PCIC projections using a delta approach (Chen et al., 2011a; Quilbé et al., 2008). In total, two emissions scenarios (i.e., RCP 2.6 and RCP 8.5) in an ensemble of five GCMs (see Table S4) were incorporated for future projection of snow depth under two downscaling techniques, and a set of 1000 simulations generated using SWAT-EBM and SWAT-TIM based on the range of input parameters were sampled to run them for the 2040–2064 period (see section 3.4).

3. Methodology

3.1. Hydrologic model

SWAT is a process-based, semi-distributed, eco-hydrological model which simulates various physical processes and their inter-connections on a daily basis (Arnold et al., 1998, 2012). Hydrological variables that are modelled in SWAT include streamflow, snow accumulation, snowmelt, infiltration, evapotranspiration, vegetation growth and canopy development, groundwater recharge and base flow, among others (Neitsch et al., 2011). SWAT has been previously applied to simulate snowmelt and snowpack in numerous studies (e.g., Debele et al., 2010; Fuka et al., 2012; Peak and Resort, 2010; Pradhanang et al., 2011; Qi et al., 2017; Troin et al., 2015b; Yang et al., 2014). Also, comparison of SWAT default snowmelt module (i.e., the TIM used in this study, see Section 3.2) show more reliable snowmelt modelling in comparison with several other snowmelt modules in the literature (Verdhen et al., 2014b). Furthermore, several studies embedded EBMs into SWAT by modifying its source code, which resulted in equally reliable or better simulations of snowmelt dynamics (Debele et al., 2010; Qi et al., 2017; Verdhen et al., 2014b) than TIMs.

In SWAT, a basin is divided into several sub-basins, which are in turn subdivided into Hydrological Response Units (HRUs) as the smallest hydrological units and characterized based on soil, landuse-land cover, slope and other geospatial features. Hydrological processes are then calculated at HRU scale, and can be aggregated at sub-basin and basin levels. In this study, we delineated a total of 174 sub-basins using a 200 km^2 threshold drainage area and a 90 m × 90 m DEM, as well as a pre-

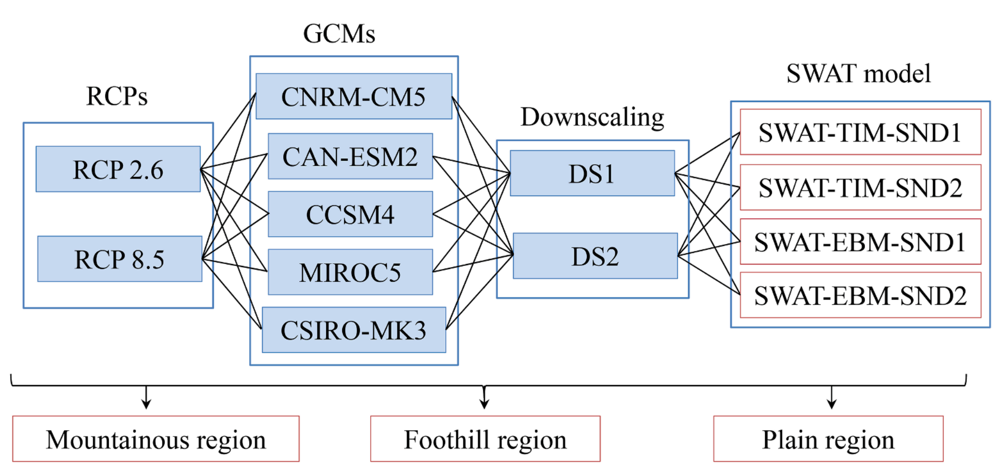

Fig. 2. Formation of SWAT models and cascades of uncertainty framework for snow depth projections. Simulations and uncertainty analysis are performed for mountainous, foothill and plain regions of the NSRB.

Table 1
Parameters used in this study and their physically meaningful ranges for snowmelt modules in SWAT-TIM and SWAT-EBM approaches.

Snowmelt module	Parameter name	Parameter description	Range	Reference
SWAT-EBM and SWAT-TIM	SFTMP	Snowfall temperature (°C)	[−5, 5]	Neitsch et al. (2011)
	TIMP	Snowpack temperature lag (°C)	[0, 1]	
SWAT-TIM	TLAPS	Temperature lapse ratio ($°C/km$)	[−10, 0]	Zhang et al. (2008); Anand et al. (2018)
	PLAPS	Precipitation lapse ratio $(mm)/km$)	[0, 250]	
	SMTMP	Snowmelt temperature (°C)	[−5, 5]	Neitsch et al. (2011)
	SMFMX	Maximum melt factor (°C)	[0, 10]	
	SMFMN	Minimum melt factor (°C)	[0, 10]	
SWAT-EBM	k_{s1}	melt coefficient parameter	[0, 2]	USACE (1998), Qi et al. (2017)
	k_{v1}	Wind control parameter	[0, 2]	
	k_{v2}	Vegetation surface dynamics parameter	[1, 5]	
	B	Snow thermal quality	[0.95, 0.97]	Dingman (2015)
	ε	Snow emissivity	[0.95, 0.99]	
	α	Snow surface albedo	[0.45, 0.85]	
	T_{ss}	Snow surface temperature (°C)	[−10, 0]	Negi et al. (2007); Singh et al. (2013); Jamieson and Schirmer (2016)

defined river network delineated previously based on a 10 m × 10 m DEM (Table S1). The 174 sub-basins were further delineated into 1639 HRUs based on soil, landuse, and slop characteristics. The daily simulation of snowmelt and snow depth was performed for each sub-basin. However, for demonstration and comparison of the model performance in snow depth simulation in mountainous, foothill, and plain regions (Fig. 1b), the monthly sub-basin data were calculated and aggregated using a weighted average of sub-basins' snow depth.

3.2. Snowmelt simulation approaches

We embeded two snowmelt simulation modules into SWAT2012 model by modifying its source code, thereby producing what we refer to as the SWAT-TIM and SWAT-EBM models. The SWAT-TIM model used in this study is the SWAT built-in snowmelt module, while the SWAT-EBM is based on the energy balance scheme developed by U.S. Army Corps of Engineers (USACE, 1998). This formulation was also embedded in the SWAT2009 by Qi et al., (2017) for simulation of snowmelt in a small catchement. For the purpose of this study, we used a similar approach as Qi et al., (2017) and embedded the modified version of EBM in the SWAT2012 by modifying its source code.

In the SWAT model, regardless of the snowmelt module used, the snowfall is stored at the ground surface in the form of snow pack. The amount of the stored snow pack is reported as SWE. The mass balance for the snow pack for day t is simulated as follows (Neitsch et al., 2011):

$$SNO_t = SNO_{t-1} + SF_t - E_{sub} - SNO_{mlt} \quad (1)$$

where SNO_t is the water content of snow pack on the ground at the end of a given day (mm H_2O), SNO_{t-1} is the water content of snowpack on the ground at the end of the previous day (mm H_2O), SF_t is the total amount of snowfall within a given day (mm H_2O), E_{sub} is the amount of sublimation on a given day (mm H_2O), and SNO_{mlt} is the amount of snowmelt within a given day (mm H_2O). SWAT considers the total precipitation for each day as snowfall if the air temperature is less than snowfall temperature (i.e., SFTMP, Table 1); otherwise, the whole precipitation is considered as rainfall. Also, the sublimation from the snow surface is calculated as a function of potential evapotranspiration of the given day. More information about the formulation of snowfall and snow sublimation can be found in Neitsch et al. (2011).

In the following, the formulations and corresponding parameters of SWAT-TIM and SWAT-EBM are discussed.

3.2.1. SWAT-TIM

In TIMs, temperature is the main driver of snowmelt. The snowmelt simulation in SWAT is based on snow cover, melt factor, and temperature variables:

$$SNO_{mlt} = b_{mlt} \cdot sno_{cov} \cdot \left[\frac{T_{snow} + T_{mx}}{2} - SMTMP \right] \quad (2)$$

where SNO_{mlt} is the amount of snowmelt on a given day (mm H_2O), b_{mlt} is the melt factor of the day (mm $H_2O \cdot day^{-1} \cdot {}^{\circ}C^{-1}$), sno_{cov} is the fraction of HRU area that is covered by snow, T_{snow} is the snowpack temperature on a given day (°C), T_{mx} is the maximum daily air temperature (°C), and $SMTMP$ is the threshold temperature at which the snowmelt will occur (°C). The melt factor for snowmelt is a function of maximum and minimum melt factor of the year and the day of the year in order to account for daily and seasonal variability of snowmelt:

$$b_{mlt} = \frac{SMFMX + SMFMN}{2} + \frac{SMFMX - SMFMN}{2} \cdot sin\left(\frac{2\pi}{365} \cdot (d_n - 81) \right) \quad (3)$$

where $SMFMX$ is the maximum melt factor of the year (mm $H_2O \cdot day^{-1} \cdot {}^{\circ}C^{-1}$); $SMFMN$ is the minimum melt factor of the year (mm $H_2O \cdot day^{-1} \cdot {}^{\circ}C^{-1}$); and d_n is the day number of the year, starting from January 1st (Neitsch et al., 2011).

The temperature dynamics of snowpack is formulated as:

$$T_{snow,t} = T_{snow,t-1} \cdot (1 - TIMP) + T_a \cdot TIMP \quad (4)$$

where $T_{snow,t}$ is the snow pack temperature on a given day (°C), $T_{snow,t-1}$ is the snow pack temperature on the previous day (°C), T_a is the average air temperature in that given day (°C), and $TIMP$ is the temperature lag factor in SWAT model (Neitsch et al., 2011). It should be noted that Equations (1) and (4) are included in both SWAT-TIM and SWAT-EBM formulations.

In order to account for the spatial variability of snowmelt process within each sub-basin in our study, five elevation bands were applied to each sub-basin in SWAT model. The elevation bands divide sub-basins into different zones based on the elevation, thereby allowing the model to discretize the hydrological processes based on sub-basins topography (Pradhanang et al., 2011). SWAT defines the temperature and precipitation of each band using the following equations:

$$P_B = P_{st} + (Z_B - Z_{st}) \times PLAPS \times 10^{-3} \quad (5)$$

$$T_B = T_{st} + (Z_B - Z_{st}) \times TLAPS \times 10^{-3} \quad (6)$$

where P_B is precipitation at elevation band (mm), P_{st} is station precipitation (mm), Z_B is midpoint elevation of band (m), Z_{st} is station elevation (m), T_B is temperature at elevation band (°C), T_{st} is station temperature (°C), $PLAPS$ is precipitation lapse rate (mm/km) and $TLAPS$ is temperature lapse rate (°C/km) (Rahman et al., 2013). In this study, TLAPS values for each sub-basin were assumed to be between −10 to 0 °C /km, and PLAPS values were defined to vary in the range 0–250

Table 2
Input data and parameters, formulations, and assumptions used in SWAT-EBM approach.

Group	Symbol	Description	Formulation
Meteorological	C_c	Cloud cover	$C_c = 1 - R_s/R_{s,max}$
	h_c	Cloud base height (m)	$h_c = 121.92 \cdot (T_a - T_d)$
	R	Rainfall (mm)	Calculated by SWAT based on SFTMP
	R_s	Solar radiation (MJm^{-2})	Input data to SWAT
	$R_{s,max}$	Daily maximum solar radiation (MJm^{-2})	Calculated by SWAT
	RH	Relative humidity	Input data to SWAT
	T_a	Average daily air temperature (°C)	Input data to SWAT
	T_c	Cloud base temperature (°C)	$T_c = TLAPS \cdot h_c + T_a$
	T_d	Dew point temperature (°C)	$T_d = T_a - 0.2 \cdot (100 - RH)$
	$TLAPS$	Temperature lapse ratio ($^{\circ}C/km$)	User defined
	v	Wind speed	Input data to SWAT
Geophysical	k_v	Wind coefficient	$k_v = k_{v1}/\exp(k_{v2} \cdot LAI)$; k_v is 1 for unforested plains and close to zero for heavily forested areas (USACE, 1998)
	k_{v1}	Calibration parameter #1 for k_v	User defined
	k_{v2}	Calibration parameter #2 for k_v	User defined
	LAI	Leaf Area Index	Calculated by SWAT
	S	Average surface slope	Calculated through GIS applications
	S_a	Average surface aspect (degree)	Calculated through GIS applications
Snowmelt	α	Snow surface albedo	User defined
	B	Snow thermal quality	User defined
	k_s	Shortwave melt coefficient	$k_s = k_{s1} \cdot [1 + sin(\pi \cdot (S_a - 90^{\circ}))S]$; k_s usually varies between 0.9 and 1.1 (USACE, 1998)
	k_{s1}	Calibration parameter for k_s	User defined
	M	Total snowmelt (mm)	Calculate through SWAT-EBM
	SNO	Snow water equivalent (mm H_2O)	Calculated through SWAT-EBM
	T_s	Snowpack temperature (°C)	Calculated through Equation (4)
	T_{ss}	Snow surface temperature	User defined
	ε	Snow emissivity	User defined

mm/km (Zhang et al., 2008; Anand et al., 2018).

In order to compute SNO_t using Equations (1) through (6), the five input parameters SMTMP, SMFMX, SMFMN, TLAPS and PLAPS need to be measured through empirical studies or calibrated. Table 1 shows the physically meaningful ranges assigned to these parameters for evaluating the performance of SWAT-TIM in snow simulations.

3.2.2. SWAT-EBM

In EBMs, the energy used for snowmelt comes from various sources including shortwave (Q_{sh}) and longwave (Q_l) net radiation, latent (Q_e) and sensible (Q_h) heat fluxes, ground heat flux (Q_g), and the energy contained in the rainfall (Q_p). Therefore, the total available energy for snowmelt (Q_m) is expressed as below (all units in $kJ.m^{-2}$):

$$Q_m = Q_{sh} + Q_l + Q_e + Q_h + Q_g + Q_p - \Delta Q_{in} \tag{7}$$

where ΔQ_{in} is the internal energy stored in snow, which includes changes in freeze and thaw processes, as well as snow temperature. This study adopted the snowmelt scheme suggested by USACE (1998) as a detailed and comprehensive EBM, which considers vegetation cover and rain-on-snow events in snowmelt modelling (Qi et al., 2017). In this snowmelt module, the amount of snowmelt for each energy component in Equation (7) is calculated as:

$$M_j = \frac{Q_j}{334.9 \cdot \rho_w \cdot B} \tag{8}$$

where M_j is the snowmelt resulted from the jth component of energy in Equation (7), i.e., Q_j ($kJ.m^{-2}$); 334.9 ($kJ.kg^{-1}$) is the latent heat of fusion of ice; ρ_w is the density of water (1000 $kg.m^{-3}$); and B is the thermal quality of snow or the fraction of ice in a unit mass of wet snow (0.95–0.97) (Gray and Landine, 1988). As a result, Equation (7) is re-written as:

$$M = M_{sh} + M_l + M_e + M_h + M_g + M_p - M_{in} \tag{9}$$

where M is the total daily snowmelt (mm), and the terms on the right side of Equation (9) are daily snowmelt values (mm) corresponded to energy sources described in Eq. (7). The USACE snowmelt module is dependent on different precipitation (i.e., rain-on-snow or rain-free) and vegetation (i.e., the value of Leaf Area Index, LAI) conditions (USACE, 1998). The equations of melt components in Equation (9) along with related parameters and data used are described in detail in USACE (1998) and Qi et al. (2017). For the sake of brevity, Table S3 shows the equations for total daily snowmelt in mm (i.e., M in Eq. (9)) based on different vegetation and precipitation conditions. Numerous parameters and input data types are required to solve the equations listed in Table S3. Table 2 shows such data and assumptions used for calculating snowmelt in SWAT-EBM. The mathematical equations outlined in Table 2 are also functions of user-defined parameters, which intensifies the role of model parameters in uncertainties of snowmelt simulations. For the purpose of this study and to examine the effect of the parameter estimation of EBM and TIM in the cascade of uncertainty for future snow depth projections, we summarized in Table 1, the physically meaningful ranges for the parameters of the SWAT-TIM and SWAT-EBM. The ranges were defined based on experiments and field measurements found in various studies in the literature. It should be noted that the ranges of k_{s1},k_{v1} and k_{v2} were defined based on the meaningful ranges of k_s and k_v values reported in USACE (1998) (see Table 1 and Table 2 and for more details). As mentioned before, the snowfall temperature and snowpack temperature lag factor were implemented in both SWAT-TIM and SWAT-EBM snowmelt modules used in this study.

3.2.3. Snow density formulation

As mentioned in previous sections, SWAT-TIM and SWAT-EBM calculate the amount of snowmelt and snow depth in the form of snow water equivalent (SWE). In order to compare SWAT results with observed snow depth data for model performance evaluation, the conversion of SWE to snow depth is necessary, which is based on SND formulations. In this study, we tested two SND formulations. The first formulation, which has already been evaluated on maritime regions of Canada (Qi et al., 2017), is referred to as SND1 in this study and is computed by:

$$SND_t = \begin{cases} SND_{t-1} + d_s \cdot (0.6 - SND_{t-1}) & \textit{no snow fall} \\ 0.1 \cdot SF_t/SNO_t + SND_{t-1}(SNO_t - SF_t)/(150 \cdot SNO_t) & \textit{snow fall} \\ SND_{t-1} + 0.5/\exp(1/M) & \textit{snow melt} \end{cases} \tag{10}$$

where SND_t is the snow density of the current day ($g.cm^{-3}$), SND_{t-1} is the snow density of the previous day ($g.cm^{-3}$), d_s is the days since the last snowfall has happened (in days), and SF_t is the snowfall of the given day.

The second snow density formulation, which has been suggested by Pomeroy et al. (1998) for Canadian Prairies, is referred to as SND2 hereafter and computed by:

$$SND_t = \begin{cases} 0.06792 + 0.05125 \cdot \exp\left(\frac{T_a}{2.59}\right) \textit{freshsnow} \\ 0.45 + \frac{20.470}{d}\left(1 - e^{-\frac{d}{673}}\right) \textit{agedsnow} \end{cases} \tag{11}$$

where T_a is the average temperature of a given day (°C), and d is the snow depth (mm). Because the snow depth of the same day is not available in SWAT before snow density is calculated, it is assumed that the d in Eq. (11) is the snow depth of the previous day. Finally, the snow depth will be calculated as:

$$D_t = \frac{SNO_t}{SND_t} \tag{12}$$

where D_t is the snow depth for day t (mm), and SND_t is calculated through Eq. 10 or Eq. (11), known as SND1 and SND2, respectively.

3.3. Performance assessment of SWAT-TIM and SWAT-EBM, and uncertainty analysis

The examination of the performance of the SWAT-TIM and SWAT-EBM models in this study are based on their ability to reproduce historical snow depth and streamflow data. The models were evaluated using monthly snow depth and streamflow measurements for the 1999–2007 and 1986–2007 periods, respectively. The comparison analyses were performed at both regional (i.e., the three regions of interest in this study including mountains, foothills, and plains) and local (i.e., 174 sub-basins) scales for snow depth simulations, and at the six hydrometric station for streamflow predictions. The inclusion of streamflow analysis in the performance assessment is because of its sensitivity to snowmelt, especially during the melt season over the April-June period. It should be noted that the main goal of this study is not to develop a calibrated hydrological model based on the best performance of snow depth simulation by comparing TIMs and EBMs. Rather, our focus is to understand robustness in model structure and uncertainties associated with using TIMs and EBMs as snowmelt modules. Hence, the observed snow depth and streamflow data were used for comparison of modelling simulation using SWAT-TIM and SWAT-EBM, and no validation in terms of snow depth and streamflow was carried out in this study. For the same reason, we did not include other influential parameters on streamflow than snowmelt related parameters (see Table 1) in our parameterization and evaluation scheme, because we opted to study only the uncertainty arising from the TIM and EBM routines not other water balance routines in the SWAT model. Therefore, for any routines other than EBM and TIM within SWAT, we relied on the model default parameters, most of which were obtained from input data such as soil database, land-use database, DEM, climate, and other data used to setup the initial SWAT models. Moreover, the streamflow simulations when only snow-related parameters were perturbed help us characterize the performance of snowmelt approaches used in this study.

Input parameters for both SWAT-TIM and SWAT-EBM were chosen based on the number of input parameters involved in TIM and EBM routines and used for snowmelt and snow depth simulations in the SWAT2012 source code (see Tables 1 and 2). For model runs and for the purpose of uncertainty analysis, we used the widest physically meaningful range for each parameter that was found from literature (Table 1). Further, we used a Latin Hypercube Sampling Technique with the Sequential Uncertainty Fitting (SUFI-2) algorithm (Abbaspour, 2015) to generate 1000 samples of parameter sets from these ranges, and fed them into the models to perform 1000 simulations for each model. For computational efficiency, we parallelized our simulations in a 200-core supercomputer using an algorithm that some authors of this study developed in earlier work (Du et al., 2020).

To evaluate the goodness-of-fit of each SWAT run, the monthly observed and simulated snow depth were compared and evaluated using three widely-used criteria of efficiency, i.e., coefficient of determination (R^2), Nash-Sutcliffe (NS), and bR^2. While NS accounts for normalized variance of observed and simulated data, bR^2 is a slope weighted coefficient of determination that considers both under- or over-predictions (using the factor “b”) and dynamics (through R^2) of data (Krause et al., 2005). Detailed formulation and their description of these criteria with relevant references are provided in Table S5. For comparison of observed and simulated values of snow depth, a sub-basin scale analysis and a regional analysis were performed. In sub-basin scale analysis, for uncertainty assessment of SWAT parameters in each sub-basin, the simulated data of sub-basins had to correspond to their closest gridded data points of observed snow depth. To do so, the observed snow depth for each sub-basin was assigned from the average of the CMC data points located within a 12-km (i.e., half of grid size) distance of each sub-basin border. After that, the simulated results and the assigned observed values of snow depth to each sub-basin were compared. For regional analysis, snow depth simulations for each sub-basin were weight-averaged over the area of the three regions of study (i.e., mountainous, foothill or plain regions), where the weight of each sub-basin was its area; then, the weight-averaged snow depth was compared with average observed snow depth acquired from gridded data for the same region (see Fig. 1b).

In addition to the efficiency criteria corresponding to the optimal parameter set among 1000 simulations in each model, we used two other statistical factors using SUFI-2, namely p-factor and r-factor for the analysis of model uncertainty. These two factors evaluate model uncertainty arising from the parameter inputs, observed data, and model structure. The p-factor varies from 0 to 1 and it shows the percentage of measured data bracketed within the uncertainty band that is predicted by model in response to the range of parameters, e.g., 1000 samples of parameter set, provided as input. The uncertainty band in SUFI-2 is calculated as the 95 percent of the cumulative distribution of the simulated variables (Abbaspour, 2015), defined as 95 Percent Prediction Uncertainty (95PPU) hereafter. While the r-factor, which varies from 0 to ∞, represents the width of the predicted uncertainty band. The ideal values for p-factor and r-factor are 1 and 0, however due to the uncertainty related to data, model structure, and input parameters such values are not achievable in regional hydrological modeling.

In this study, comparison and performance assessment of the SWAT-TIM and SWAT-EBM models were not only based on the best performing set of parameters from a total of 1000 simulations, but also uncertainty analysis based on p-factor and r-factor. It is suggested that for streamflow simulations, values between 0.6 and 0.8 for p-factor and values around 1.0 for r-factor show a reasonable performance for streamflow simulation in areas at the scale of our study watershed (Abbaspour, 2015). Overall, we performed a total of 80,000 simulations with 40,000 for each of the SWAT-TIM and SWAT-EBM models (i.e., 40,000 = 1000 parameter samples × 5 GCMs × 2 RCPs × 2 Downscaling techniques × 2 SNDs), albeit by parallelizing in a 200-core computer (see Fig. 2).

3.4. Uncertainty decomposition and spatiotemporal apportionment

For quantifying the cascade of uncertainty associated with future projection of snow depth using SWAT-EBM and SWAT-TIM approaches, we used the ANOVA method, which has been successfully carried out in various studies, including hydrological studies (e.g., Déqué et al., 2007; Yip et al., 2011). The ANOVA method decomposes the projected variance and attributes its parts to different uncertainty sources and their interactions. In this study, the sources of uncertainty incorporated in ANOVA include hydrologic model parameterization (95PPU), GCMs, RCPs, and Downscaling methods (DS). According to the statistical theory of ANOVA, the total sum of squares (SST) is calculated as the sum of the variations resulting from each uncertainty source, and from their interactions. As a result, the SST for this study is defined as (Wang et al., 2018):

$$SST = SS_{GCM} + SS_{RCP} + SS_{DS} + SS_{95PPU} + SSI \tag{13}$$

where SS_{GCM} is the uncertainty share of GCMs, SS_{RCP} is the uncertainty share of RCPs, SS_{DS} is the uncertainty share of downscaling methods, SS_{95PPU} is the uncertainty share of SWAT-EBM and SWAT-TIM model parameters, and SSI is the uncertainty resulting from interactions of uncertainty sources from all different combinations of two, three, and four variables (i.e., 95PPU, GCM, RCP, and DS):

$$\begin{aligned} SSI = {} & SS_{GCM*RCP} + SS_{GCM*DS} + SS_{GCM*95PPU} + SS_{RCP*DS} + SS_{RCP*95PPU} \\ & + SS_{DS*95PPU} + SS_{GCM*RCP*DS} + SS_{GCM*RCP*95PPU} + SS_{GCM*DS*95PPU} \\ & + SS_{RCP*DS*95PPU} + SS_{GCM*RCP*DS*95PPY} \end{aligned} \tag{14}$$

SSI shows the interaction effect of uncertainty components on the variability of snow depth. Therefore, high contributions of SSI to uncertainty cascade suggests non-additive effect of GCMs, RCPs, DSs, and 95PPU on snow depth dynamics. For more details see Bosshard et al. (2013).

In this study, a combination of 40 scenarios were applied to each of SWAT-TIM and SWAT-EBM in order to compare the share of uncertainty sources in the total cascade of uncertainty projection for snow depth projections (Fig. 2). The monthly variation of the cascade of uncertainty projections were projected across the study area and the results were discussed for the three main regions, i.e., mountains, foothills, and plains, over the study watershed.

4. Results and discussion

4.1. Model performance of snow depth simulations at sub-basin scale

Fig. 3 shows the sub-basin scale results of snow depth simulations related to the four combinations of SWAT models (i.e., SWAT-TIM, SWAT-EBM, SND1, and SND2). Based on the results shown in Fig. 3a, the parameter ranges defined in both SWAT-TIM and SWAT-EBM had a moderate performance in reproducing observed snow depth data, although it is shown that SWAT-TIM was able to have a slightly higher value of average p-factor, therefore slightly better performance as compared to EBM, especially in plain areas. It is shown in Fig. 3a that the change of snow density formulation had a considerable effect on p-factor values, particularly in foothill and plain regions. It is however clear that none of snowmelt modules under either of the two snow density

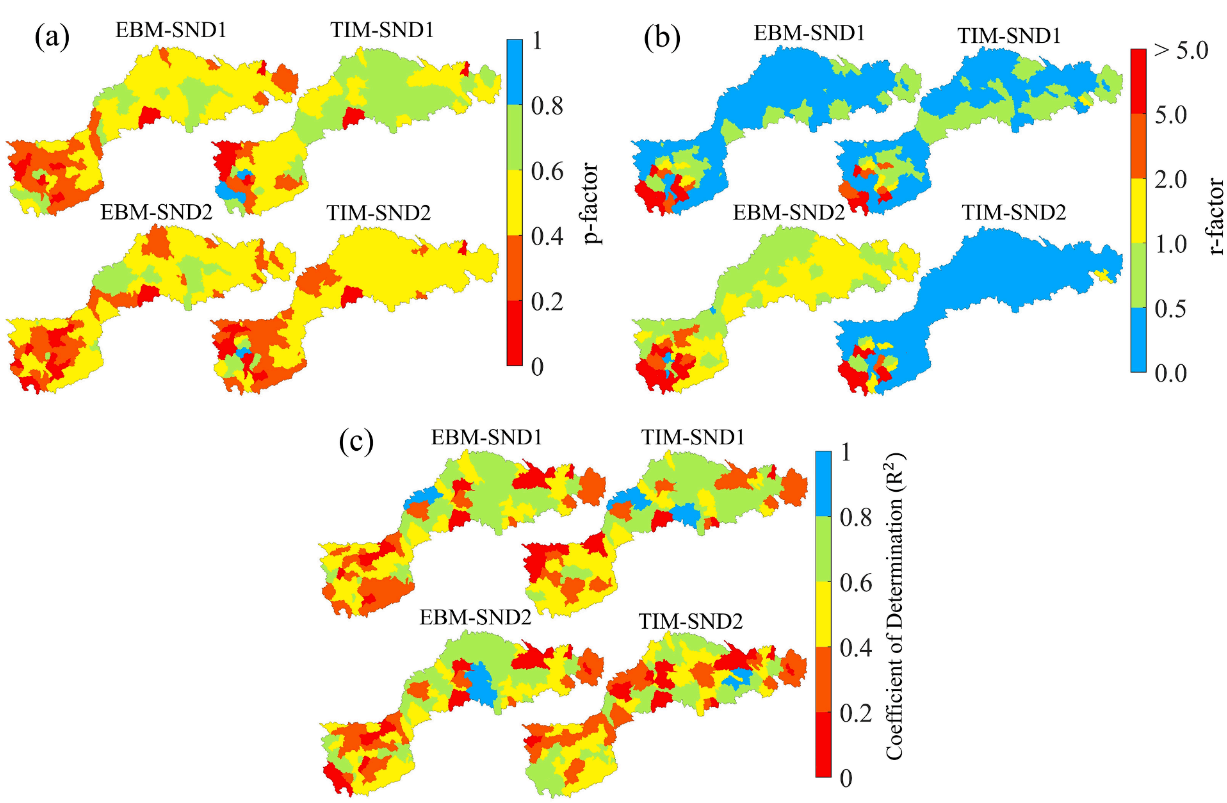

Fig. 3. Results of (a) p-factor, (b) r-factor and (c) best R^2 calculated based on 1000 simulations of monthly snow depth using combinations of SWAT-EBM and SWAT-TIM with SND1 and SND2 for 1999–2007 period.

Table 3
Maximum, minimum, and average values of p-factors, r-factors and R^2 for sub-basins within different regions of NSRB.

		SND1						SND2					
		TIM			EBM			TIM			EBM		
		max	min	avg.	max	min	avg.	max	min	avg.	max	min	avg.
Mountains	p	0.85	0.06	0.45	0.71	0.00	0.37	0.82	0.04	0.35	0.73	0.00	0.34
	r	12.8	0.16	2.07	42.7	0.15	6.09	71.1	0.09	9.12	138.5	0.40	20.28
	R^2	0.76	0.08	0.39	0.75	0.09	0.40	0.77	0.18	0.49	0.75	0.09	0.40
Foothills	p	0.73	0.32	0.59	0.65	0.27	0.46	0.56	0.27	0.44	0.64	0.19	0.46
	r	0.63	0.21	0.43	0.78	0.17	0.38	0.47	0.05	0.20	2.15	0.45	1.06
	R^2	0.78	0.09	0.45	0.70	0.12	0.45	0.77	0.14	0.46	0.70	0.12	0.45
Plains	p	0.75	0.14	0.60	0.73	0.08	0.47	0.58	0.17	0.46	0.71	0.14	0.45
	r	1.03	0.16	0.50	0.68	0.25	0.39	1.04	0.00	0.15	1.93	0.64	1.08
	R^2	0.80	0.00	0.55	0.85	0.03	0.51	0.81	0.01	0.45	0.85	0.03	0.51

approaches had adequately reproduced historical snow depth in mountainous regions. The average p-factors shown in Table 3 and Fig. 3 represent the lower level of performance for mountainous regions for any snow depth simulation approaches than the other two regions. This highlights the complexity of snow-related processes in mountainous regions, which is exacerbated by the lack of reliable and consistent climate data in such areas. The noticeable temporal gaps in precipitation time series, as well as their inadequate spatial coverage in mountainous regions are potentially a major reason for the poor performance of snowmelt modules to simulate snow depths in mountainous regions (Mizukami et al., 2014; Ul Islam and Déry, 2017). On the other hand, the spatial variability of temperature (which affects both SWAT-EBM and SWAT-TIM simulations), and solar radiation, wind speed and relative humidity (which affects SWAT-EBM simulations only), in mountainous regions is higher than that in foothill and plain regions. Therefore, the coarse spatial resolutions of such climate data compared to their actual topographic variability in mountainous regions (see Table S2) may be another reason for the low performance of SWAT-TIM and SWAT-EBM in simulating historical snow depth data in most of sub-basins within mountainous region (Comola et al., 2015; Helbig et al., 2015; DeBeer and Pomeroy, 2017). Another issue regarding the usage of gridded climate data is that the dependencies between important climate variables such as precipitation and temperature are not commonly maintained in gridded datasets, which might result in biases in reproducing hydrological responses such as snow accumulation and melt (Singh and Reza Najafi, 2020). It should be noted that temperature and precipitation are the only climate input data used in both SWAT-TIM and SWAT-EBM. Therefore, the poor performance of both modules in mountainous regions (see Fig. 3 and Fig. 4) suggests the upmost importance of temperature and precipitation data, rather than solar radiation, humidity and wind speed (which are inputs to SWAT-EBM only).

Fig. 4 shows the variation of monthly p-factors of snow depth analysis based on different sub-basins within mountainous, foothill and plain regions. It is shown that in most of the months, the p-factors of sub-basins across mountainous regions had the largest variability compared to those of plain and foothill regions. Nevertheless, the average values of p-factor within mountainous regions were lower than those of foothill and plain regions (see Fig. 4 and Table 3). While none of the four model combinations shown in Fig. 4 can be presented as superior to others in terms of reproducing historical snow depth, the

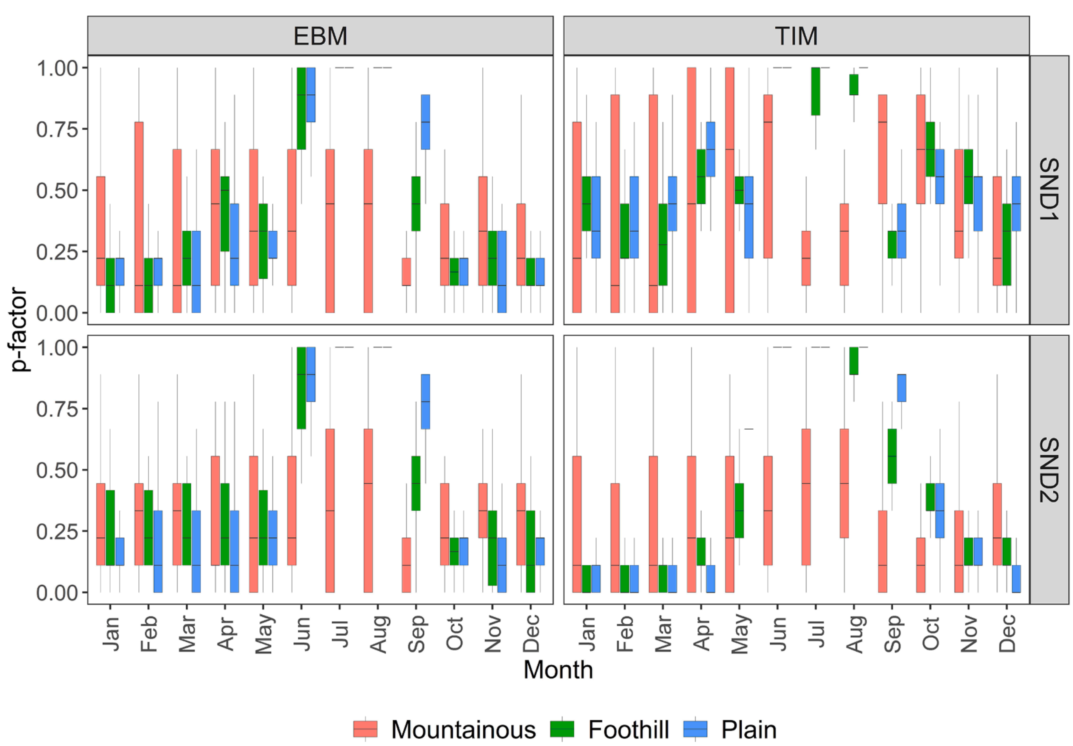

Fig. 4. Monthly variation of the p-factor values within three regions of NSRB using four snow depth simulation approaches. The box plots show the range of p-factors obtained across sub-basins.

changes in p-factor ranges under different approaches were noticeable (e.g., changes from TIM-SND1 to TIM-SND2). It is also noteworthy that in Fig. 4, the variability of p-factor in foothill and plain regions during summer months was negligible, since foothill and plain areas of NSRB usually had minimum or no snow cover during summer.

Overall, the high variability of p-factors using both TIM and EBM and under both SND1 and SND2 in mountainous region suggest unreliable snow depth simulation as a result of complex topography and lack of adequate and reliable climate datasets, even when a more comprehensive model structure (e.g., EBM combinations) is utilized (Helbig et al., 2015).

Fig. 3b shows the r-factors corresponded to historical snow depth simulations of NSRB sub-basins. The high value of r-factor for several sub-basins in mountainous regions suggests that the effect of snow parameters in simulating snow depth can be significant in mountainous regions with high topographic and climate variability. This can be particularly related to areas with complex and highly variable hydrology, as the average and maximum values of r-factor in the non-mountainous region is noticeably smaller than those within the mountainous region. It can be interpreted from Table 3 that the average values of r-factors in mountainous regions were considerably greater than other areas, where the average p-factor values were less than those in other areas. These results are consistent with findings of Najafi and Moradkhani (2015). High r-factor and low p-factor in mountainous region implies that a larger uncertainty is predicted in this area, where only small share of the historic data were reproduced using any of the two models under any of the SND combinations. Since EBMs are more physically-based approaches by definition than TIMs are, the poor performance of EBM models under any of the SND combinations are likely due to the poor quality of input data, i.e., spatiotemporal climate factors and input parameters used to run them. This suggests a clear need for enhancement of data collection and monitoring strategies within mountainous regions (Clow et al., 2012; Helbig et al., 2015; DeBeer and Pomeroy, 2017) than enhancement of the modelling approaches themselves. The uncertainty range (i.e., r-factor) of mountainous regions of EBMs in both SND1 and SND2 was higher than those in TIMs, suggesting that the effect of model parameterization on modelling uncertainty of snow depth simulations is intensified in complex areas (i.e., mountainous regions in this study) (Ul Islam and Déry, 2017). On the other hand, the r-factors of snow depth simulation in all regions under EBM-SND2 were increased compared to the r-factors related to EBM-SND1, with the highest level of difference within mountainous regions (see Table 3).

The additional modelling uncertainty resulting from using SND2 instead of SND1 could be attributed to two factors: First, the major difference between SND1 and SND2 is significance of air temperature in SND2 formulation. According to Eq. (11), under fresh snow (i.e., snowfall) conditions, snow density is solely a function of current air temperature. On the other hand, under aged snow conditions, snow density is a function of snow depth of the previous day, a variable that is calculated based on the snow density of the previous day. As a result, the snow density under SND2 is a strong function of air temperature of a given day or its previous day(s). Therefore, it can be argued that incorporating air temperature factor in snow density estimation resulted in more uncertainty in snow depth simulations using SND2. Second, SND1 is mostly dependent on outputs of daily simulations of snowmelt modules such as SND of the previous day, snowfall, and days after last snow; on the other hand, SND2 contains more empirical parameters that are determined based on observed site data within Canadian Prairies (Pomeroy et al., 1998). Since such empirical parameters are not case-specific (e.g., they are not specific to NSRB), the SND2 may be less representative of physical processes in our study watershed. This might contribute to the higher uncertainty resulting from using SND2 as snow density function.

Finally, our analysis of the R^2 values corresponding to the best simulation results (out of 1000 model runs) is shown in Fig. 3c. An overview of the results from four different model-SND combination shows that, in general, the snow depth in sub-basins of plain areas were simulated properly, yet demanding improvements. Although some sub-basins in the plain region had the R^2 of less than 0.4, most of the sub-basins showed a R^2 value of 0.6 or above, which can be an indicator of a proper snowpack simulation in plain areas. The comparison of observed and simulated snow depth data in the foothill and mountainous regions, however, showed poorer results compared to those of plain regions. Although sporadic sub-basins with a proper R^2 can be found in foothill and mountainous regions, most of the sub-basins showed the R^2 value of less than 0.6. This can be due to the likely error inherent in the gridded snow depth data used for our comparison, as well as their coarse resolution (i.e., 24 km × 24 km) for sub-basin-based comparison (Vaughan, 2013; Helbig et al., 2015). In other words, the comparison of simulated and observed data for sub-basins was based on assigning the historical data from coarse resolution grid points to each sub-basins. Hence, the spatial heterogeneity of historical snow depth are under-represented at the sub-basin scale. For the same reason, we are not presenting NS and bR^2 results of snow depth simulation, since they provide more detailed comparison of the simulated versus observed data, which require a higher resolution measurements for a direct and comprehensive assessment. Furthermore, the lack of time-series data for precipitation in regions with high variability in topography and climate such as west side of NSRB resulted in a poorer model performance (Mizukami et al., 2014; Ul Islam and Déry, 2017). Consequently, presentation of comparison results at a regional-scale in our study would give more reliable insights than those of sub-basin scale.

4.2. Effect of snow density formulation on model performance at regional scale

The results in this section reveal the effect of snow density formulation on performance and uncertainty associated with simulations and projections of snow depth. The results of the best model runs out of 1000 simulations for various regions, snowmelt approaches (EBM, TIM), and snow depth approaches (SND1 and SND2) are shown in Fig. 5 and Table S6. As shown in Fig. 5a, when using SND1, neither the SWAT-TIM (with an average NS, bR^2, and R^2 of 0.45, 0.19, 0.65) nor the SWAT-EBM (NS, bR^2, and R^2 of 0.51, 0.23, 0.66) could reliably simulate the dynamics and magnitudes of regional snow depth within the mountainous regions of NSRB. However, by implementing SND2, which is an empirical formulation specifically meant for Canadian Prairies (Pomeroy et al., 1998), a considerable improvement in simulation of regional snow depth in both SWAT-TIM (with an average NS, bR^2, and R^2 of 0.79, 0.58, 0.80) and SWAT-EBM (NS, bR^2, and R^2 of 0.25, 0.69, 0.78) can be seen. Comparison of Fig. 5a with Fig. 5b and 5c reveals that the proper formulation of snow density function plays an important role in quantifying snow depth, particularly in mountainous regions (Sturm et al., 2010; Bormann et al., 2013). In fact, higher variability of snow depth within mountainous regions along with high variability of temperature might be the reason why the snow depth in such regions is more sensitive to definition of snow density formulations. Results of daily snow density over the simulation period (1983–2007) for all sub-basins show an average of 275 kg/m^3 with standard deviation of 169 kg/m^3 for SND1, and an average of 154 kg/m^3 with standard deviation of 91 kg/m^3 for SND2. This shows variable results for snow density in different times and locations. Estimations from SND1 are higher than observed snow density values in Alberta (Pavlovskii et al., 2019), and also in Canadian Prairies, especially for fresh snow events (Pomeroy and Brun, 2001; Pomeroy et al., 1998). On the other hand, the performance of SWAT-TIM and SWAT-EBM under SND1 and SND2 in snow depth simulation within foothills and plains were nearly the same. Nevertheless, it is detected that SWAT-EBM-SND2, which is known to be more physically based and robust in snow depth simulation, mostly overestimated the snow depth in all the regions within NSRB. The overestimation of snow depth can be a result of overestimation of SWE, underestimation of snow density, or a

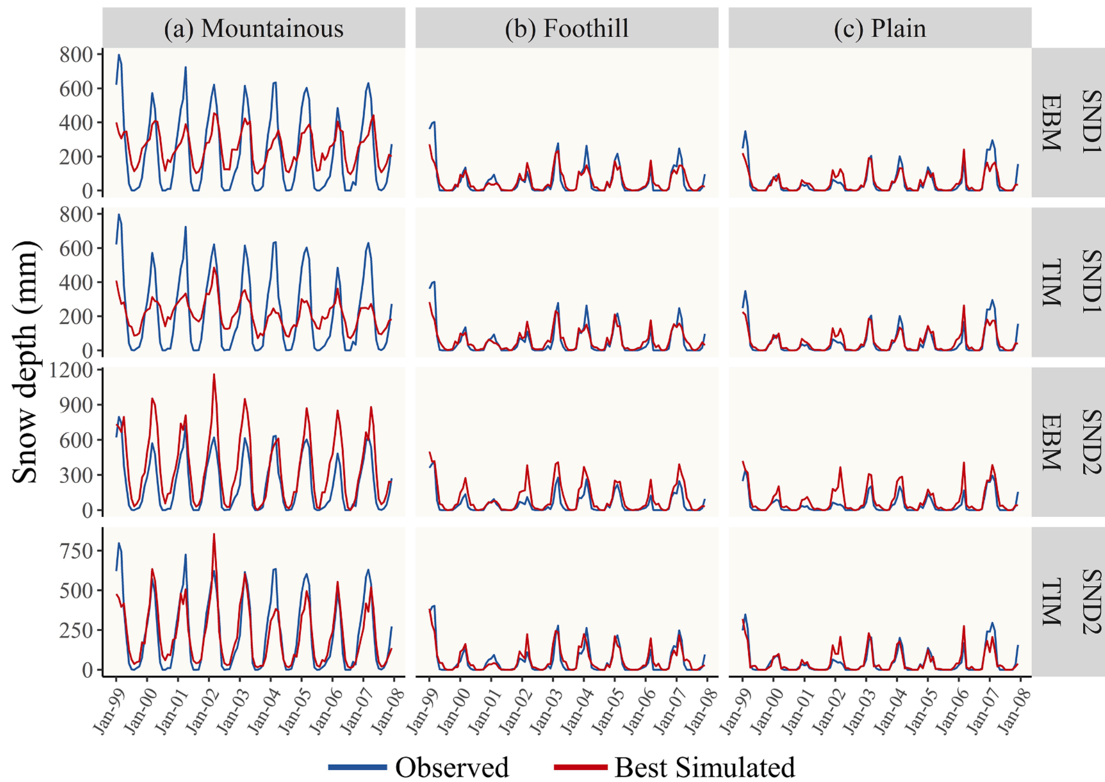

Fig. 5. Comparison of the best simulated (i.e., best results out of 1000 SWAT simulations) snow depth (red) with observed (blue) data in (a) mountainous, (b) foothill and (c) plain regions for the 1999–2007 period.

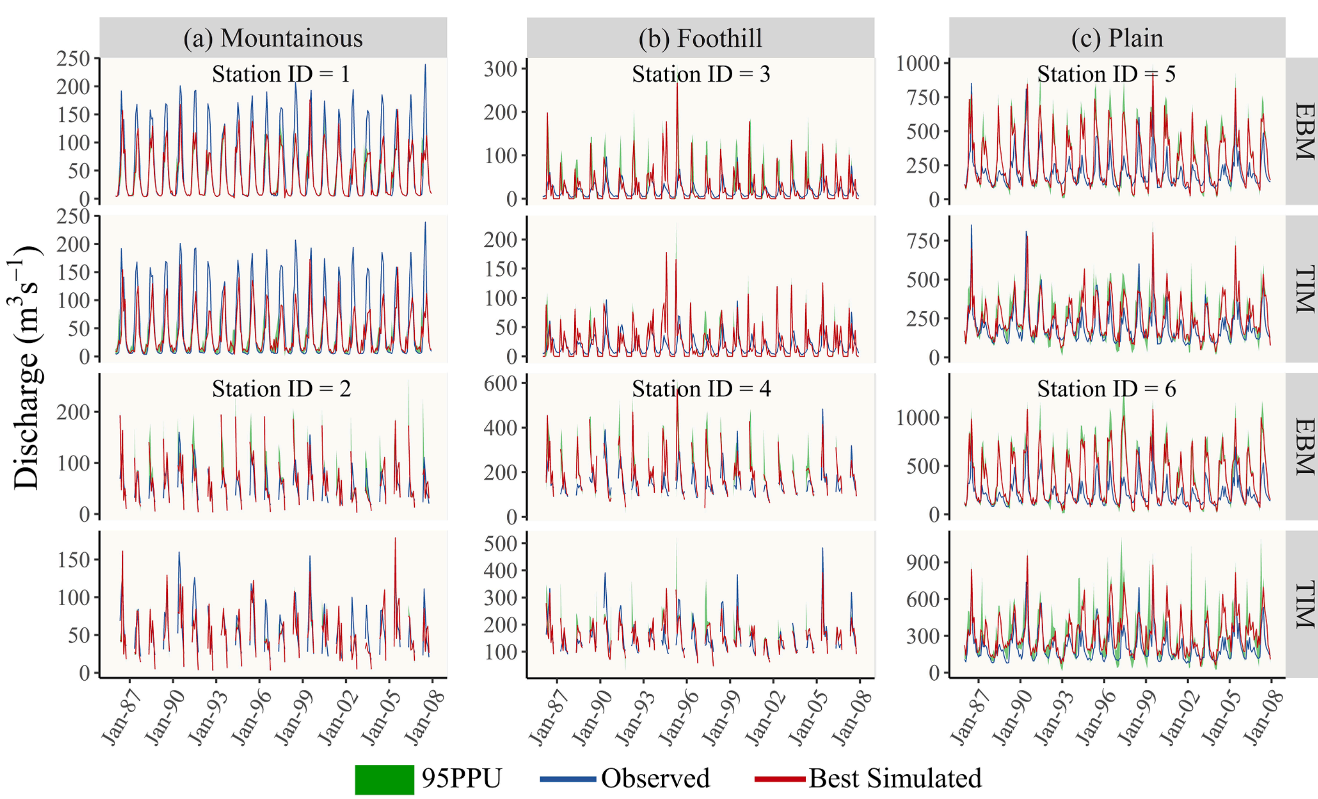

Fig. 6. Comparison of monthly observed (blue), best simulated (red), and 95PPU (green band) streamflow for 1986–2007 period using SWAT-EBM (left column) and SWAT-TIM (right column). 95PPU: 95 percent prediction uncertainty.

combination of those. It can be seen in Fig. 6 (Section 4.3) that EBMs have overestimated streamflow on the main tributary of NSR, which can be partially inter-related to overestimation of SWE in such areas and their upstream regions.

4.3. Assessment of SWAT-TIM and SWAT-EBM in reproducing streamflow

Since streamflow is a function of snowmelt in terms of SWE (rather than snow depth), SWE is independent from SND approaches used. Hence, streamflow reproduction results in this section are reported in terms of SWAT-TIM and SWAT-EBM approaches, because using SND1 or SND2 has no effect on streamflow values. The streamflow simulation using 1000 parameter set samples in SWAT-EBM and SWAT-TIM shows that in the upstream stations (see Fig. 1 and Table S1), representing Mountainous region, with p-factors of 0.57 and 0.33 for stations #1 and #2 respectively, the SWAT-EBM performed slightly better than SWAT-TIM with p-factor of 0.40 and 0.16 for stations #1 and #2, respectively (Table 4). In terms of NS and bR^2 SWAT-EBM with NS of 0.66 and bR^2 of 0.42 performed slightly better than SWAT-TIM with NS of 0.59 and bR^2 of 0.34 in station #1; however, the performance of SWAT-TIM was much better in station #2, with NS of 0.23 and bR^2 of 0.27 for SWAT-TIM as compared to NS of -1.43 and bR^2 of 0.05 from SWAT-EBM simulations (see Table 4). On the other hand, SWAT-TIM had performed marginally better in simulating streamflow data within downstream hydrometric stations. Comparisons of the r-factor, NS and bR^2 shows relatively close values for SWAT-TIM and SWAT-EBM within both mountainous and plain regions, suggesting that the performance of TIM and EBM within a large watershed with diverse hydro-climate and topographic conditions was relatively similar in simulating the streamflow dynamics. These results are in line with previous studies on comparison of TIMs and EBMs for streamflow simulations (Franz et al., 2008; Zhang et al., 2008; Zeinivand and De Smedt, 2009; Debele et al., 2010; Meng et al., 2017). One important point, however, is the low values of NS of SWAT-EBM in most of the hydrometric stations. It is found in the literature that the EBMs might overestimate the streamflow due to overestimation of mid-winter SWE (Franz et al., 2008). As it can be found from the comparison of EBM and TIM in Fig. 6, the best performing simulation results of EBM, out of 1000 simulations, was yet overestimating the peak flows, resulting in low values of NS, which highlighted the constant overestimation of the flow (Krause et al., 2005, see Table 4). It is noteworthy that the streamflow simulations are based on best-fitting snow parameters only, and the other parameters related to soil, groundwater, and runoff that are sensitive to streamflow can be adjusted in order to change the simulated streamflow results in Fig. 6, which is beyond the scope of this study. Nevertheless, the overestimation of peak flow resulting from using SWAT-EBM is noticeable (i.e., within hundreds of cubic meter per second), which might not be rectified by logical adjustment of other SWAT parameters. As a result, the potential overestimation of streamflow through using EBMs should be taken into account in hydrological studies such as analyzing extreme conditions (i.e., floods and droughts) throughout regional studies.

4.4. Evaluation of uncertainty sources in the cascade of uncertainty projection

The average monthly results of uncertainty decomposition for snow depth projection in mountainous, foothill, and plain regions are shown in Fig. 7. Also, the annual average values of contributions of different uncertainty sources for the same regions is outlined in Table S7. It can be seen from the figures that the share of parameter uncertainty within all regions of NSRB is considerable, although holding different values in different regions and times. A general comparison of cascades of uncertainty of mountainous, foothill, and plain regions based on Fig. 7 and Table S7 shows that 95PPU arising from SWAT-EBM and SWAT-TIM holds the largest share of uncertainty in mountainous regions, compared to foothill and plain regions. This uncertainty range was resulted from 1000 set of parameter combination sampled from a physically meaningful range defined from literature (see Table 1). This suggest the importance of model parameterization and the input data in complex regions for snow depth simulations and projections (Mizukami et al., 2014; Ul Islam and Déry, 2017). As we move from mountainous to foothill and plain regions, the average annual share of parameter uncertainty becomes less than that of mountainous regions as the share of annual PPU, under NSD2, changes from 75.4% and 57.0% for EBM and TIM, respectively in mountainous to 57.8% and 42.1% in foothill, and to 59%, and 27.5% in plain region, respectively (see Table S7). In the Mountainous region and under SND1 and SND2 formulations, both SWAT-TIM and SWAT-EBM showed a relatively similar trend in sharing the formation of cascade of uncertainty. The average value of 95PPU contribution to cascade of uncertainty for EBM-SND1, TIM-SND1 and TIM-SND2 ranges between 55% and 60%, presenting a relatively similar behavior of parameter uncertainty within these approaches. The average parameter uncertainty from EBM-SND2, however, is 75%, which suggests the noticeable effect of snow density approach in the formation of cascade of uncertainty in EBM model. EBM-SND2 also holds the largest share of parameter uncertainty for foothill and plain regions. It is also shown in Fig. 7a that the share of parameter uncertainty decreased in warmer seasons (i.e., May to August). This indicates that as the weather gets warmer in mountainous regions, the effect of various GCMs, RCPs, downscaling methods and their interactions on snow depth projections increased, since they directly affect the precipitation, air temperature and solar radiation, which are major drivers of snowmelt and snow depth, therefore forcing a larger variation in projection of snowfall and therefore snow depth than hydrologic model parameters. On the other hand, snowfall events are less frequent in warm seasons (MacDonald et al., 2012), which makes the effect of snowmelt parameters within EBM and TIM less than those for colder

Table 4
Performance of average monthly streamflow simulation for SWAT-TIM and SWAT-EBM for 1986–2007.

Region	Station ID (Table S2)	Snowmelt module	p-factor	r-factor	R^2	NS	bR^2
Mountains	1	EBM	0.57	0.16	0.72	0.66	0.42
		TIM	0.40	0.13	0.69	0.59	0.34
	2	EBM	0.33	0.82	0.10	−1.43	0.05
		TIM	0.16	0.17	0.41	0.23	0.27
Foothills	3	EBM	0.14	0.93	0.14	−3.74	0.13
		TIM	0.08	0.28	0.18	−1.70	0.13
	4	EBM	0.34	0.76	0.21	−1.22	0.14
		TIM	0.40	0.39	0.39	0.34	0.21
Plains	5	EBM	0.23	0.49	0.57	−0.65	0.47
		TIM	0.36	0.46	0.66	0.44	0.56
	6	EBM	0.29	0.72	0.61	−2.04	0.40
		TIM	0.36	0.78	0.57	−0.10	0.52

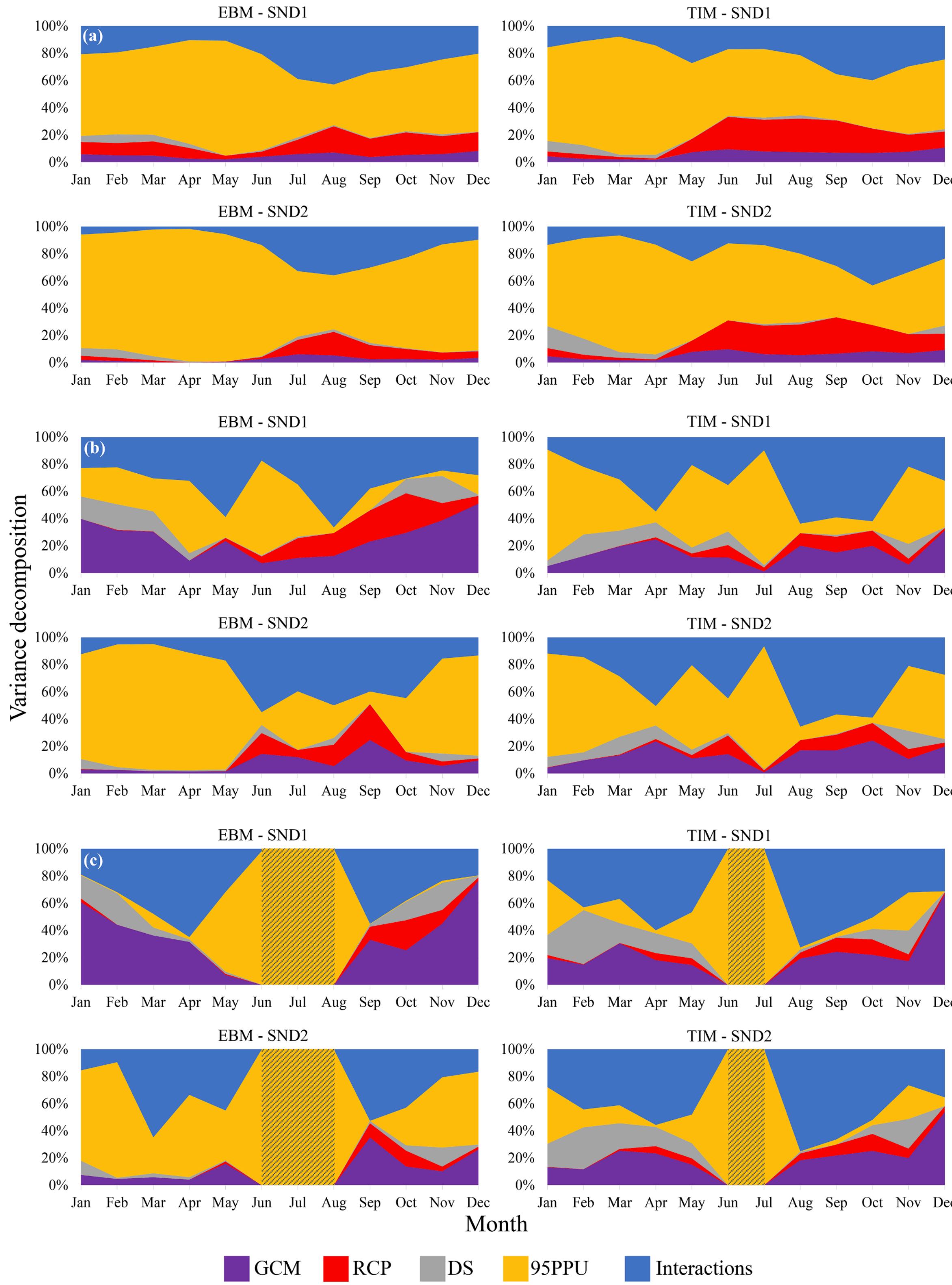

Fig. 7. Variance decomposition of the uncertainty in snow depth projection within (a) mountainous, (b) foothill, and (c) plain regions throughout NSRB using SWAT-TIM and SWAT-EBM under SND1 and SND2 for future climate (2040–2064). Note: diagonal lines indicate times when snow depth is meager and 95PPU numerically gains maximum share in ANOVA analysis.

seasons. As a result, the effect of GCMs, RCPs, downscaling methods and their interactions was increased in warm seasons. In colder seasons, however, GCMs, RCPs, downscaling methods and their interactions had less contribution to the cascade of uncertainty in mountainous regions, possibly because temperature variability is less effective of snow formation in cold seasons. In cold seasons, the air temperature within mountainous regions are well below freezing point; therefore, the variability of temperature among various GCMs, RCPs and downscaling methods does not effect the conversion of precipitation to snowfall or rainfall. Because of that, EBM and TIM parameter uncertainty controls most of the uncertainty associated with snow depth simulations in these months than the GCMs, RCPs, and DS. As the study region changes from mountainous areas to foothill and plain regions, the share of different uncertainty sources varies for different months. The comparison of Fig. 7a, b and c shows that by shifting from mountainous to plain regions, the contribution of parameter uncertainty to cascade of uncertainty decreased, while other sources of uncertainty contributed more to the overall uncertainty of snow depth projections. In particular, the contribution of GCM to the uncertainty cascade increased from mountainous region to foothill and plain regions. This is an interesting finding as it provides insight into the conflicting assessments in the literature with some studies concluded GCMs as the largest contributor to the uncertainty projection (Prudhomme and Davies, 2009; Vetter et al., 2017) and others introduced emission scenarios (Vetter et al., 2015), and fewer studies underscored the effects of hydrologic models (Ashraf Vaghefi et al., 2019) in the cascade of uncertainty projections. Our study provides a comprehensive assessment of all contributing factors across spatial and temporal scales and under diverse hydro-climatic and topographic conditions, and it describes how changes from mountainous to plain regions result in different pattern in the share of uncertainty contribution. Same as warm months within mountainous regions, the increased share of GCM uncertainty in foothill and plain regions in comparison with mountainous regions might be partially related to the effect of air temperature on considering precipitation as snowfall or rainfall in SWAT model (see Section 3.2). Furthermore, since the parameter uncertainty had decreased from mountainous to foothill and plain regions (Fig. 7), this mathematically resulted in the share of other uncertainty sources to increase, which is possibly one other reason for the increase of GCM contribution to uncertainty cascades in foothill and plain regions. The contribution of interactions of different uncertainty sources is the second most important contributor to the cascade of uncertainty of mountainous regions and among the largest contributors in foothill and plain regions, suggesting the non-linear effect of uncertainty sources on snow depth projections (Chawla and Mujumdar, 2018).

Another important point to mention is related to the contribution of model parameter uncertainty to the cascade of uncertainty within plain regions in warm months (i.e., May to August), which is close to 100%, while this contribution is much lower in other months of the year (Fig. 7c). The large contribution of model parameters to the cascade of uncertainty in warmer months is due to the high temperature of plain regions in warm months. The temperature of this region is significantly higher than the snowfall temperature (especially in June, July and August), which makes the snowfall to rarely happen, therefore resulting in a zero contribution of GCM, RCP, and DS. On the other hand, the amount of snow depth in warm months is almost zero, as almost all the snow depth has been melted throughout the spring (e.g., April and May). As a result, a meager change in snow depth simulation right before or during the warm months will numerically result in a large variance calculation for the 95PPU, using ANOVA method, as compared to the small value of snow depth. As presented with diagonal lines in Fig. 7c, due to the zero share of GCM, RCP, and DS during warm months in plain region, the 95PPU gained the maximum share of the uncertainty despite its negligible variation due to the parameter uncertainty.

5. Conclusion, study limitations, and future directions

Snowmelt and snow depth processes are among the most significant hydrological processes in most of high elevation watersheds in the northern latitudes and mountainous watersheds with cold hydrology. However, the contribution of uncertainty due to the use of Temperature Index Modules (TIMs) and Energy Balance Modules (EBMs) in projection of snowmelt and snow depth in regional studies is poorly understood. We implemented the ANOVA uncertainty decomposition approaches, where a process-based TIM and EBM snowmelt routines, as well as two different snow density modules were coupled within the Soil and Water Assessment Tool (SWAT) source code and future projections were performed based on an ensemble climate datasets of five GCMs, under the two future scenarios of RCP 2.6 and RCP 8.5 and using two downscaling approaches. This allowed spatiotemporal assessment of the uncertainty projections of snowmelt and snow depth across heterogeneous landscapes, from mountainous and foothill to plain areas using a large river basin in Alberta, western Canada as the study region. The main conclusions of this study are:

1. The performance of EBM and TIM approaches in simulating snowmelt and snow depth is different across scales and time; therefore, conclusions from a small-scale study with a homogeneous landscape and hydro-climate condition cannot be generalized to a regional scale and for a longer period of time.
2. While the performances of EBM and TIM were relatively similar in mountainous regions and both produced a relatively large uncertainty, the spatiotemporal analysis of the p-factor, r-factor, NSE, bR^2, and R^2 indicated that SWAT-TIM performed better in foothill and plain regions as compared to the SWAT-EBM combinations and the SWAT-EBM approach overestimated streamflow in most regions and snow depth in all the regions within the study watershed.
3. While snowmelt simulation modules are key in hydrologic modelling of snow dominated regions, the performance of the models in snow depth simulations is more dependent on the formulation of snow density simulation, rather than using TIM or EBM. This highlights the importance of the selection of a proper snow density (SND) approach in accordance with the study area and climatic conditions.
4. All EBM, TIM, SND1, and SND2 model combinations predicted larger uncertainty in simulation of snow depth and streamflow in the mountainous regions as compared to foothill and plain areas. Since EBMs are a more physically-based approach by definition than TIMs, the poor performance of SWAT-EBM model under any of the SND combinations are likely due to the poor quality of input data, i.e., spatiotemporal climate factors and input parameters used to run them. This observation suggests a clear need for enhancement of data collection and monitoring strategies within mountainous regions.
5. The analysis of the cascade of uncertainty for future snow depth simulation indicated that the share of uncertainty from different sources varies over time and across regions. While the share of uncertainty was dominated by EBM and TIM parameterization in the highland areas and in cold months, it was conquered by the GCMs, RCPs, and DS in lower elevation foothill and plain areas. The share of uncertainty was also affected by the choice of snow density approach, and the SWAT-EBM-SN2 modeling approach resulted in a larger share of uncertainty in future snow depth projection, due to a more physically-based nature of the model combination, as compared to all other model combinations.
6. The larger share of parameter uncertainty in cold months is related to the air temperature that are well below freezing point making the variability of temperature among various GCMs, RCPs and downscaling methods ineffective in the conversion of precipitation to snowfall or rainfall in the mountainous regions, while the larger parameter uncertainty in warm months in the plain regions is related to a significantly higher than the snowfall temperature, which makes the snowfall to rarely happen, therefore resulting in a zero contribution of GCM, RCP, and DS and numerically allocating a large uncertainty share to the parameters.

This research facilitates better understanding of the performance and uncertainties associated with the projection of snowmelt and snow depth using EBM and TIM approaches in regional studies, where hydro-climate and geospatial features vary across regions and times. It also demonstrates that a multi-scale and temporal analysis is needed for understanding the cascade of uncertainties in future snowmelt and snow depth simulations. Our study underscores the importance of the input climate data in simulation of hydrological processes in the high elevation areas that is likely more significant than the choice of model structure and process representation. Furthermore, regional station-based observed data do not represent the average snow depth within a large region of study (i.e., with scales of hundreds of square kilometers), a fact that highlights the need of proper spatial gridded data for comparison of snow depth simulations. On the other hand, the gridded data of historical snow depth or SWE within Canadian Prairies are scarce, and it is difficult to acquire proper gridded data for snow depth at a fine spatial resolution. Hence, any improvement in historical climate data such as precipitation and temperature, as well as historical snow depth data can result in an improved quality of snowmelt and snow depth analysis within large regions. Such improvements may also change the spatiotemporal patterns of uncertainty sources in snow depth projections, possibly as a result of more reliable data in regions with complex hydrology. Therefore, we suggest these analysis to be applied on other study regions with a rich climate data status, in order to examine the importance of input climate data in simulations and projections of snowmelt and/or snow depth.

It is worth mentioning that our analysis of the cascade of uncertainty was performed for future snow depth projections. A more comprehensive uncertainty analyses for hydrologic water balance components and streamflow can provide more insights about the uncertainty decomposition across study area. In addition, future projections in our study did not simulate operation of reservoirs in the future and it considered daily historical outflow of the two main dams in the study watershed. Although it did not affect our uncertainty analyses of the snow depth and snowmelt projections in this study, and since simulation of reservoir operations was beyond the scope of this study, a realistic reflection of future management and decisions on operation of dams and reservoirs in the hydrologic model can add another layer of uncertainty which can be studied for a more comprehensive assessment of the uncertainty in streamflow and hydrologic simulations.

Moreover, while our results suggested that the uncertainties in EBM and TIM can dominate the overall uncertainties, a more robust analyses of uncertainty decomposition by considering more members of GCMs and RCPs and DS techniques, as well as examining other EBM and TIM approaches used in literature can provide more improved understanding of the cascade of uncertainty. Furthermore, the performance and uncertainty of applying different SND approaches can be examined by (1) applying other widely-used SND functions to the appropriate study region; and (2) refining suitable SND equations through optimizing and readjusting their empirical parameters based on the observed data from the study region.

Credit authorship contribution statement

Majid Zaremehrjardy: Data curation, Formal analysis, Methodology, Software, Validation, Visualization, Writing - original draft, Writing - review & editing. **Saman Razavi:** Writing - review & editing. **Monireh Faramarzi:** Supervision, Conceptualization, Formal analysis, Writing - review & editing, Project administration, Funding acquisition.

Declaration of Competing Interest

The authors declare that they have no known competing financial interests or personal relationships that could have appeared to influence the work reported in this paper.

Acknowledgements

We would like to thank Dr. Junyu Qi for guiding us about EBM formulations and operation within SWAT model. Funding for this study has been received from Campus Alberta Innovation Program Chair (Grant# RES0034497), and Natural Sciences and Engineering Research Council of Canada Discovery Grant (Grant# RES0043463).

Appendix A. Supplementary data

Supplementary data to this article can be found online at https://doi.org/10.1016/j.jhydrol.2020.125735.

References

Abbas, T., Hussain, F., Nabi, G., Boota, M.W., Wu, R.-S., 2019. Uncertainty evaluation of SWAT model for snowmelt runoff in a Himalayan watershed. Terr. Atmos. Ocean. Sci. 30 (2), df. https://doi.org/10.3319/TAO.2018.10.08.01.

Abbaspour, K.C., 2015. SWAT-CUP: SWAT Calibration and Uncertainty Programs- A User Manual, Department of Systems Analysis, Intergrated Assessment and Modelling (SIAM),EAWAG. Swiss Federal Institute of Aqualtic Science and Technology, Duebendorf, Switzerland. Doi: 10.1007/s00402-009-1032-4.

Aggarwal, S.P., Thakur, P.K., Nikam, B.R., Garg, V., 2014. Integrated approach for snowmelt run-off estimation using temperature index model, remote sensing and GIS. Curr. Sci. 106, 397–407.

Ahmadalipour, A., Moradkhani, H., Rana, A., 2018. Accounting for downscaling and model uncertainty in fine-resolution seasonal climate projections over the Columbia River Basin. Clim Dyn 50 (1-2), 717–733.

Alberta Environment and Parks, 2019. Alberta river basins [WWW Document]. accessed 7.30.19. https://web.archive.org/web/20160409210242/http://www.environment.alberta.ca/apps/basins/default.aspx.

Ammar, M.E., Gharib, A., Islam, Z., Davies, E.G.R., Seneka, M., Faramarzi, M., 2020. Future floods using hydroclimatic simulations and peaks over threshold: An alternative to nonstationary analysis inferred from trend tests. Adv. Water Resour. 136, 103463. https://doi.org/10.1016/j.advwatres.2019.103463.

Anand, J., Gosain, A.K., Khosa, R., Srinivasan, R., 2018. Regional scale hydrologic modeling for prediction of water balance, analysis of trends in streamflow and variations in streamflow: The case study of the Ganga River basin. J. Hydrol.: Reg. Stud. 16, 32–53.

Arnold, J., Moriasi, D., Gassman, P., Abbaspour, K., White, M., Srinivasan, R., Santhi, C., Harmel, R., van Griensven, A., Van Liew, M., Kannan, N., Jha, M., 2012. SWAT: Model Use, Calibration, and Validation. Trans. ASABE 55, 1317–1335. https://doi.org/10.13031/2013.42244.

Arnold, J., Srinivasan, R., Muttiah, R., Williams, J., 1998. Large Area Hydrologic Modeling and Assessment; Part I: Model Development. J. Am. Water Resour. Assoc. 17, 73. https://doi.org/10.1016/S0899-9007(00)00483-4.

Ashraf Vaghefi, S., Iravani, M., Sauchyn, D., Andreichuk, Y., Goss, G., Faramarzi, M., 2019. Regionalization and parameterization of a hydrologic model significantly affect the cascade of uncertainty in climate-impact projections. Clim Dyn 53 (5-6), 2861–2886.

Avanzi, F., De Michele, C., Ghezzi, A., 2015. On the performances of empirical regressions for the estimation of bulk snow density. Geogr. Fis. Dinam. Quat. 38, 105–112. https://doi.org/10.4461/GFDQ.2015.38.10.

Barnhart, T.B., Molotch, N.P., Livneh, B., Harpold, A.A., Knowles, J.F., Schneider, D., 2016. Snowmelt rate dictates streamflow: Snowmelt Rate Dictates Streamflow. Geophys. Res. Lett. 43 (15), 8006–8016.

Bavera, D., Bavay, M., Jonas, T., Lehning, M., De Michele, C., 2014. A comparison between two statistical and a physically-based model in snow water equivalent mapping. Advances in Water Resources 63, 167–178.

Beven, K., Freer, J., 2001. Equifinality, data assimilation, and uncertainty estimation in mechanistic modelling of complex environmental systems using the GLUE methodology. J. Hydrol. 249 (1-4), 11–29.

Bocchiola, D., Groppelli, B., 2010. Spatial estimation of snow water equivalent at different dates within the Adamello Park of Italy. Cold Reg. Sci. Technol. 63 (3), 97–109.

Bormann, K.J., Westra, S., Evans, J.P., McCabe, M.F., 2013. Spatial and temporal variability in seasonal snow density. J. Hydrol. 484, 63–73.

Bosshard, T., Carambia, M., Georgen, K., Kotlarski, S., Krahe, P., Zappa, M., Schar, C., 2013. Quantifying uncertainty sources in an emsemble of hydrological climate-impact projections. Water Resour. Res. 49, 1523–1536. https://doi.org/10.1007/s00704-017-2359-3.

Brown, R.D., Bransnett, B. 2010. Canadian Meteorological Centre (CMC) Daily Snow Depth Analysis Data, Version 1. [WWW Document]. Boulder, Colorado USA. NASA National Snow and Ice Data Center Distributed Active Archive Center. https://doi.org/10.5067/W9FOYWH0EQZ3.

Bürger, G., Sobie, S.R., Cannon, A.J., Werner, A.T., Murdock, T.Q., 2013. Downscaling extremes: An intercomparison of multiple methods for future climate. Journal of Climate 26, 3429–3449. https://doi.org/10.1175/JCLI-D-12-00249.1.

Cannon, A.J., 2015. Selecting GCM scenarios that span the range of changes in a multimodel ensemble: Application to CMIP5 climate extremes indices. Journal of Climate 28, 1260–1267. https://doi.org/10.1175/JCLI-D-14-00636.1.

Chawla, I., Mujumdar, P.P., 2018. Partitioning uncertainty in streamflow projections under nonstationary model conditions. Adv. Water Resour. 112, 266–282.

Chen, J., Brissette, F.P., Leconte, R., 2011a. Uncertainty of downscaling method in quantifying the impact of climate change on hydrology. J. Hydrol. 401 (3-4), 190–202.

Chen, J., Brissette, F.P., Poulin, A., Leconte, R., 2011b. Overall uncertainty study of the hydrological impacts of climate change for a Canadian watershed. Water Resour. Res. 47, 1–16. https://doi.org/10.1029/2011WR010602.

Clow, D.W., Nanus, L., Verdin, K.L., Schmidt, J., 2012. Evaluation of SNODAS snow depth and snow water equivalent estimates for the Colorado Rocky Mountains, USA. Hydrol. Process. 26, 2583–2591. https://doi.org/10.1002/hyp.9385.

Comola, F., Schaefli, B., Ronco, P.D., Botter, G., Bavay, M., Rinaldo, A., Lehning, M., 2015. Scale-dependent effects of solar radiation patterns on the snow-dominated hydrologic response. Geophys. Res. Lett. 42 (10), 3895–3902.
DeBeer, C.M., Pomeroy, J.W., 2017. Influence of snowpack and melt energy heterogeneity on snow cover depletion and snowmelt runoff simulation in a cold mountain environment. J. Hydrol. 553, 199–213.
Debele, B., Srinivasan, R., Gosain, A.K., 2010. Comparison of Process-Based and Temperature-Index Snowmelt Modeling in SWAT. Water Resour Manage 24 (6), 1065–1088.
Déqué, M., Rowell, D.P., Lüthi, D., Giorgi, F., Christensen, J.H., Rockel, B., Jacob, D., Kjellström, E., de Castro, M., van den Hurk, B., 2007. An intercomparison of regional climate simulations for Europe: assessing uncertainties in model projections. Clim. Change 81 (S1), 53–70.
Dingman, L., 2015. Physical Hydrology. Waveland Press.
Do, N.C., Razavi, S., 2020. Correlation Effects? A Major but Often Neglected Component in Sensitivity and Uncertainty Analysis. Water Resour. Res. 56 (3) https://doi.org/10.1029/2019WR025436.
Du, X., Loiselle, D., Alessi, D.S., Faramarzi, M., 2020. Hydro-climate and biogeochemical processes control watershed organic carbon inflows: Development of an in-stream organic carbon module coupled with a process-based hydrologic model. Sci. Total Environ. 718, 137281. https://doi.org/10.1016/j.scitotenv.2020.137281.
Fang, X., Pomeroy, J.W., Westbrook, C.J., Guo, X., Minke, A.G., Brown, T., 2010. Prediction of snowmelt derived streamflow in a wetland dominated prairie basin. Hydrol. Earth Syst. Sci. 14 (6), 991–1006. https://doi.org/10.5194/hess-14-991-2010.
Faramarzi, M., Abbaspour, K.C., Adamowicz, W.L.(., Lu, W., Fennell, J., Zehnder, A.J.B., Goss, G.G., 2017. Uncertainty based assessment of dynamic freshwater scarcity in semi-arid watersheds of Alberta, Canada. J. Hydrol.: Reg. Stud. 9, 48–68.
Faramarzi, M., Abbaspour, K.C., Schulin, R., Yang, H., 2009. Modelling blue and green water resources availability in Iran. Hydrol. Process. 26, 1–16. https://doi.org/10.1002/hyp.
Faramarzi, M., Srinivasan, R., Iravani, M., Bladon, K.D., Abbaspour, K.C., Zehnder, A.J.B., Goss, G.G., 2015. Setting up a hydrological model of Alberta: Data discrimination analyses prior to calibration. Environ. Modell. Software 74, 48–65.
Ficklin, D.L., Barnhart, B.L., 2014. SWAT hydrologic model parameter uncertainty and its implications for hydroclimatic projections in snowmelt-dependent watersheds. J. Hydrol. 519, 2081–2090.
Franz, K.J., Hogue, T.S., Sorooshian, S., 2008. Operational snow modeling: Addressing the challenges of an energy balance model for National Weather Service forecasts. J. Hydrol. 360 (1-4), 48–66.
Fu, C., James, A.L., Yao, H., 2015. Investigations of uncertainty in SWAT hydrologic simulations: A case study of a Canadian Shield catchment. Hydrol. Process. 29, 4000–4017. https://doi.org/10.1002/hyp.10477.
Fuka, D.R., Easton, Z.M., Brooks, E.S., Boll, J., Steenhuis, T.S., Walter, M.T., 2012. A Simple Process-Based Snowmelt Routine to Model Spatially Distributed Snow Depth and Snowmelt in the SWAT Model. J. Am. Water Resour. Assoc. 48, 1151–1161. https://doi.org/10.1111/j.1752-1688.2012.00680.x.
Government of Canada, 2019. Historical Climate Data [WWW Document]. URL http://climate.weather.gc.ca/historical_data/search_historic_data_e.html (accessed 8.6.19).
Gray, D.M., Landine, P.G., 1988. An energy-budget snowmelt model for the Canadian Prairies. Can. J. Earth Sci. 25 (8), 1292–1303.
Haghnegahdar, A., Razavi, S., Yassin, F., Wheater, H., 2017. Multicriteria sensitivity analysis as a diagnostic tool for understanding model behaviour and characterizing model uncertainty. Hydrol. Process. 31 (25), 4462–4476.
Harder, P., Helgason, W.D., Pomeroy, J.W., 2018. Modeling the Snowpack Energy Balance during Melt under Exposed Crop Stubble. Journal of Hydrometeorology 19, 1191–1214. https://doi.org/10.1175/jhm-d-18-0039.1.
Helbig, N., van Herwijnen, A., Magnusson, J., Jonas, T., 2015. Fractional snow-covered area parameterization over complex topography. Hydrol. Earth Syst. Sci. 19 (3), 1339–1351. https://doi.org/10.5194/hess-19-1339-2015.
Hock, R., 2003. Temperature index melt modelling in mountain areas. J. Hydrol. 282 (1-4), 104–115.
Islam, S. ul, Déry, S.J., Werner, A.T., 2017. Future Climate Change Impacts on Snow and Water Resources of the Fraser River Basin, British Columbia. Journal of Hydrometeorology 18, 473–496. https://doi.org/10.1175/jhm-d-16-0012.1.
Jamieson, B., Schirmer, M., 2016. Measuring snow surface temperature: why, why not, and how?.
Jonas, T., Marty, C., Magnusson, J., 2009. Estimating the snow water equivalent from snow depth measurements in the Swiss Alps. J. Hydrol. 378 (1-2), 161–167.
Jost, G., Weiler, M., Gluns, D.R., Alila, Y., 2007. The influence of forest and topography on snow accumulation and melt at the watershed-scale. J. Hydrol. 347 (1-2), 101–115.
Jung, I.-W., Moradkhani, H., Chang, H., 2012. Uncertainty assessment of climate change impacts for hydrologically distinct river basins. J. Hydrol. 466-467, 73–87.
Kim, Y., Ohn, I., Lee, J.-K., Kim, Y.-O., 2019. Generalizing uncertainty decomposition theory in climate change impact assessments. Journal of Hydrology X 3, 100024. https://doi.org/10.1016/j.hydroa.2019.100024.
Krause, P., Boyle, D.P., Bäse, F., 2005. Comparison of different efficiency criteria for hydrological model assessment. Adv. Geosci. 5, 89–97. https://doi.org/10.5194/adgeo-5-89-2005.
Li, H., Wang, Z., He, G., Man, W., 2017. Estimating Snow Depth and Snow Water Equivalence Using Repeat-Pass Interferometric SAR in the Northern Piedmont Region of the Tianshan Mountains. J. Sens. 2017, 1–17.
Liu, W., Wang, L., Sun, F., Li, Z., Wang, H., Liu, J., Yang, T., Zhou, J., Qi, J., 2018. Snow Hydrology in the Upper Yellow River Basin Under Climate Change: A Land Surface Modeling Perspective. J. Geophys. Res.: Atmosph. 123, 12676–12691. https://doi.org/10.1029/2018JD028984.
MacDonald, R.J., Byrne, J.M., Boon, S., Kienzle, S.W., 2012. Modelling the Potential Impacts of Climate Change on Snowpack in the North Saskatchewan River Watershed, Alberta. Water Resour Manage 26 (11), 3053–3076.
Mas, A., Baraer, M., Arsenault, R., Poulin, A., Préfontaine, J., 2018. Targeting high robustness in snowpack modeling for Nordic hydrological applications in limited data conditions. J. Hydrol. 564, 1008–1021.
Massmann, C., 2019. Modelling Snowmelt in Ungauged Catchments. Water 11 (2), 301. https://doi.org/10.3390/w11020301.
Masud, M., Ferdous, J., Faramarzi, M., 2018. Projected Changes in Hydrological Variables in the Agricultural Region of Alberta, Canada. Water 10 (12), 1810. https://doi.org/10.3390/w10121810.
McCreight, J.L., Small, E.E., 2014. Modeling bulk density and snow water equivalent using daily snow depth observations. The Cryosphere 8 (2), 521–536. https://doi.org/10.5194/tc-8-521-2014.
McKenney, D.W., Hutchinson, M.F., Papadopol, P., Lawrence, K., Pedlar, J., Campbell, K., Milewska, E., Hopkinson, R.F., Price, D., Owen, T., 2011. Customized Spatial Climate Models for North America. Bull. Amer. Meteor. Soc. 92 (12), 1611–1622.
Meng, T., Carewa, R., Florkowski, W.J., Klepacka, A.M., 2017. Analyzing temperature and precipitation influences on yield distributions of canola and spring wheat in Saskatchewan. J. Appl. Meteorol. Climatol. 56, 897–913. https://doi.org/10.1175/JAMC-D-16-0258.1.
Mizukami, N., Clark, M.P., Slater, A.G., Brekke, L.D., Elsner, M.M., Arnold, J.R., Gangopadhyay, S., 2014. Hydrologic implications of different large-scale meteorological model forcing datasets in mountainous regions. J. Hydrometeorol. 15, 474–488. https://doi.org/10.1175/JHM-D-13-036.1.
Mizukami, N., Perica, S., 2008. Spatiotemporal characteristics of snowpack density in the mountainous regions of the Western United States. J. Hydrometeorol. https://doi.org/10.1175/2008JHM981.1.
Najafi, M.R., Moradkhani, H., 2015. Multi-model ensemble analysis of runoff extremes for climate change impact assessments. J. Hydrol. 525, 352–361.
Najafi, M.R., Zwiers, F., Gillett, N., 2017. Attribution of the observed spring snowpack decline in British Columbia to anthropogenic climate change. Journal of Climate. https://doi.org/10.1175/JCLI-D-16-0189.1.
Negi, H.S., Thakur, N.K., Mishra, V.D., 2007. Estimation and validation of snow surface temperature using modis data for snow-avalanche studies in NW-Himalaya. J. Indian Soc. Remote Sens. 35 (4), 287–299.
Neitsch, S., Arnold, J., Kiniry, J., Williams, J., 2011. Soil & Water Assessment Tool Theoretical Documentation Version 2009. Texas Water Resources Institute 1–647. https://doi.org/10.1016/j.scitotenv.2015.11.063.
North Saskatchewan Watershed Alliance, 2005. The State of the North Sask River Watershed Report.
Pavlovskii, I., Hayashi, M., Itenfisu, D., 2019. Midwinter melts in the Canadian prairies: energy balance and hydrological effects. Hydrol. Earth Syst. Sci. 23 (4), 1867–1883. https://doi.org/10.5194/hess-23-1867-2019.
Peak, J., Resort, M., 2010. Using SWAT Model and Snow Survey Data to Assess Spatial Variability of Snowpack in the Cannonsville Watershed , New 73–85.
Pomeroy, J., Brun, E., 2001. Physical Properties of Snow Introduction: Snow Physics and Ecology, in: Snow Ecology.
Pomeroy, J.W., Gray, D.M., Shook, K.R., Toth, B., Essery, R.L.H., Pietroniro, A., Hedstrom, N., 1998. An evaluation of snow accumulation and ablation processes for land surface modelling. Hydrol. Process. 12, 2339–2367. https://doi.org/10.1002/(SICI)1099-1085(199812)12:15<2339::AID-HYP800>3.0.CO;2-L.
Poulin, A., Brissette, F., Leconte, R., Arsenault, R., Malo, J.-S., 2011. Uncertainty of hydrological modelling in climate change impact studies in a Canadian, snow-dominated river basin. J. Hydrol. 409 (3-4), 626–636.
Pradhanang, S.M., Anandhi, A., Mukundan, R., Zion, M.S., Pierson, D.C., Schneiderman, E.M., Matonse, A., Frei, A., 2011. Application of SWAT model to assess snowpack development and streamflow in the Cannonsville watershed, New York, USA. Hydrol. Process. 25, 3268–3277. https://doi.org/10.1002/hyp.8171.
Prudhomme, C., Davies, H., 2009. Assessing uncertainties in climate change impact analyses on the river flow regimes in the UK. Part 2: future climate. Clim. Change 93 (1-2), 197–222.
Qi, J., Li, S., Jamieson, R., Hebb, D., Xing, Z., Meng, F.-R., 2017. Modifying SWAT with an energy balance module to simulate snowmelt for maritime regions. Environ. Modell. Software 93, 146–160.
Quilbé, R., Rousseau, A.N., Moquet, J.-S., Trinh, N.B., Dibike, Y., Gachon, P., Chaumont, D., 2008. Assessing the Effect of Climate Change on River Flow Using General Circulation Models and Hydrological Modelling – Application to the Chaudière River, Québec, Canada. Canadian Water Resour. J. 33 (1), 73–94.
Rahman, K., Maringanti, C., Beniston, M., Widmer, F., Abbaspour, K., Lehmann, A., 2013. Streamflow Modeling in a Highly Managed Mountainous Glacier Watershed Using SWAT: The Upper Rhone River Watershed Case in Switzerland. Water Resour Manage 27 (2), 323–339.
Raleigh, M.S., Clark, M.P., 2014. Are temperature-index models appropriate for assessing climate change impacts on snowmelt? Proc. 82nd Western Snow Conference 45–51.
Raleigh, M.S., Livneh, B., Lapo, K., Lundquist, J.D., 2016. How does availability of meteorological forcing data impact physically based snowpack simulations? J. Hydrometeorol. 17, 99–120. https://doi.org/10.1175/JHM-D-14-0235.1.
Razavi, S., Gupta, H.V., 2019. A multi-method Generalized Global Sensitivity Matrix approach to accounting for the dynamical nature of earth and environmental systems models. Environ. Modell. Software 114, 1–11.
Razavi, S., Tolson, B.A., Matott, L.S., Thomson, N.R., MacLean, A., Seglenieks, F.R., 2010. Reducing the computational cost of automatic calibration through model

preemption. Water Resour. Res. 46, 1–17. https://doi.org/10.1029/2009WR008957.

Renard, B., Kavetski, D., Kuczera, G., Thyer, M., Franks, S.W., 2010. Understanding predictive uncertainty in hydrologic modeling: The challenge of identifying input and structural errors. Water Resour. Res. 46, 1–22. https://doi.org/10.1029/2009WR008328.

Shrestha, R.R., Dibike, Y.B., Prowse, T.D., 2012. Modelling of climate-induced hydrologic changes in the Lake Winnipeg watershed. J. Great Lakes Res. 38, 83–94.

Singh, H., Reza Najafi, M., 2020. Evaluation of gridded climate datasets over Canada using univariate and bivariate approaches: Implications for hydrological modelling. J. Hydrol. 584, 124673. https://doi.org/10.1016/j.jhydrol.2020.124673.

Singh, K.K., Mishra, V.D., Singh, D.K., Ganju, A., 2013. Estimation of snow surface temperature for NW Himalayan regions using passive microwave satellite data. Indian J. Radio Space Phys. 42, 27–33.

Singh, V.P., Frevert, D.K., 2002. Mathematical Models of Large Watershed Hydrology. Water Resour. Publications.

Sobol', I.M., 1993. Sensitivity Estimates for Nonlinear Mathematical Models. Mathematical Modeling and Computational experiment. https://doi.org/1061-7590/93/04407-008.

Sturm, M., Taras, B., Liston, G.E., Derksen, C., Jonas, T., Lea, J., 2010. Estimating snow water equivalent using snow depth data and climate classes. Journal of Hydrometeorology 11, 1380–1394. https://doi.org/10.1175/2010JHM1202.1.

Sun, Ning, Yan, Hongxiang, Wigmosta, Mark S., Leung, L. Ruby, Skaggs, Richard, Hou, Zhangshuan, 2019. Regional Snow Parameters Estimation for Large-Domain Hydrological Applications in the Western United States. J. Geophys. Res. Atmos. 124 (10), 5296–5313.

Taylor, K.E., Stouffer, R.J., Meehl, G.A., 2012. An overview of CMIP5 and the experiment design. Bull. Am. Meteorol. Soc. 93, 485–498. https://doi.org/10.1175/BAMS-D-11-00094.1.

Tiwari, S., Kar, S.C., Bhatla, R., Bansal, R., 2018. Temperature index based snowmelt runoff modelling for the Satluj River basin in the western Himalayas. Meteorol. Appl. 25, 302–313. https://doi.org/10.1002/met.1692.

Tobin, Cara, Schaefli, Bettina, Nicótina, Ludovico, Simoni, Silvia, Barrenetxea, Guillermo, Smith, Russell, Parlange, Marc, Rinaldo, Andrea, 2013. Improving the degree-day method for sub-daily melt simulations with physically-based diurnal variations. Adv. Water Resour. 55, 149–164.

Todd Walter, M., Brooks, Erin S., McCool, Donald K., King, Larry G., Molnau, Myron, Boll, Jan, 2005. Process-based snowmelt modeling: does it require more input data than temperature-index modeling? J. Hydrol. 300 (1-4), 65–75.

Troin, Magali, Arsenault, Richard, Brissette, François, 2015a. Performance and Uncertainty Evaluation of Snow Models on Snowmelt Flow Simulations over a Nordic Catchment (Mistassibi, Canada). Hydrology 2 (4), 289–317. https://doi.org/10.3390/hydrology2040289.

Troin, Magali, Caya, Daniel, Velázquez, Juan Alberto, Brissette, François, 2015b. Hydrological response to dynamical downscaling of climate model outputs: A case study for western and eastern snowmelt-dominated Canada catchments. J. Hydrol.: Reg. Stud. 4, 595–610.

Ul Islam, Siraj, Déry, Stephen J., 2017. Evaluating uncertainties in modelling the snow hydrology of the Fraser River Basin, British Columbia, Canada. Hydrol. Earth Syst. Sci. 21 (3), 1827–1847. https://doi.org/10.5194/hess-21-1827-2017.

USACE, 1998. Runoff From Snowmelt. Engineering and Design 142.

van Vuuren, Detlef P., Edmonds, Jae, Kainuma, Mikiko, Riahi, Keywan, Thomson, Allison, Hibbard, Kathy, Hurtt, George C., Kram, Tom, Krey, Volker, Lamarque, Jean-Francois, Masui, Toshihiko, Meinshausen, Malte, Nakicenovic, Nebojsa, Smith, Steven J., Rose, Steven K., 2011. The representative concentration pathways: an overview. Clim. Change 109 (1-2), 5–31.

Vaughan, D.G., 2013. Observations: cryosphere Climate Change 2013: The Physical Science Basis. Climate Change 2013 the Physical Science Basis: Working Group I Contribution to the Fifth Assessment Report of the Intergovernmental Panel on Climate Change in: T F Stocker, D Qin, G-K Plattner, M Tignor, S K Allen, J Boschung, A Nauels, Y Xia, V Bex and P. (Eds.) https://doi.org/10.1017/CBO9781107415324.012.

Verdhen, A., Chahar, B.R., Sharma, O.P., 2014a. Springtime Snowmelt and Streamflow Predictions in the Himalayan Mountains. J. Hydrol. Eng. 19 (7), 1452–1461.

Verdhen, Anand, Chahar, Bhagu R., Sharma, Om P., 2014b. Snowmelt Modelling Approaches in Watershed Models: Computation and Comparison of Efficiencies under Varying Climatic Conditions. Water Resour. Manage. 28 (11), 3439–3453.

Vetter, T., Huang, S., Aich, V., Yang, T., Wang, X., Krysanova, V., Hattermann, F., 2015. Multi-model climate impact assessment and intercomparison for three large-scale river basins on three continents. Earth Syst. Dynam. 6 (1), 17–43. https://doi.org/10.5194/esd-6-17-2015.

Vetter, Tobias, Reinhardt, Julia, Flörke, Martina, van Griensven, Ann, Hattermann, Fred, Huang, Shaochun, Koch, Hagen, Pechlivanidis, Ilias G., Plötner, Stefan, Seidou, Ousmane, Su, Buda, Vervoort, R. Willem, Krysanova, Valentina, 2017. Evaluation of sources of uncertainty in projected hydrological changes under climate change in 12 large-scale river basins. Clim. Change 141 (3), 419–433.

Wang, Bin, Liu, De Li, Waters, Cathy, Yu, Qiang, 2018. Quantifying sources of uncertainty in projected wheat yield changes under climate change in eastern Australia. Clim. Change 151 (2), 259–273.

Wilby, R.L., Harris, I., 2006. A framework for assessing uncertainties in climate change impacts: Low-flow scenarios for the River Thames, UK. Water Resour. Res. 42, 1–10. https://doi.org/10.1029/2005WR004065.

Wu, Qiaofeng, Liu, Shuguang, Cai, Yi, Li, Xinjian, Jiang, Yangming, 2017. Improvement of hydrological model calibration by selecting multiple parameter ranges. Hydrol. Earth Syst. Sci. 21 (1), 393–407. https://doi.org/10.5194/hess-21-393-2017.

Yang, Yan, Onishi, Takeo, Hiramatsu, Ken, 2014. Improving the Performance of Temperature Index Snowmelt Model of SWAT by Using MODIS Land Surface Temperature Data. Scient. World J. 2014, 1–20.

Yip, Stan, Ferro, Christopher A.T., Stephenson, David B., Hawkins, Ed, 2011. A Simple, Coherent Framework for Partitioning Uncertainty in Climate Predictions. J. Climate 24 (17), 4634–4643.

Young, K.L., Assini, J., Abnizova, A., Miller, E.A., 2013. Snowcover and melt characteristics of upland/lowland terrain: Polar bear pass, bathurst island, nunavut, Canada. Hydrol. Res. 44, 2–20. https://doi.org/10.2166/nh.2012.083.

Zeinivand, H., De Smedt, F., 2010. Prediction of snowmelt floods with a distributed hydrological model using a physical snow mass and energy balance approach. Nat. Hazards 54 (2), 451–468.

Zeinivand, H., De Smedt, F., 2009. Hydrological Modeling of Snow Accumulation and Melting on River Basin Scale. Water Resour. Manage. 23 (11), 2271–2287.

Zhang, X., Srinivasan, R., Debele, B., Hao, F., 2008. Runoff simulation of the headwaters of the yellow river using the SWAT model with three snowmelt algorithms. J. Am. Water Resour. Associat. 44, 48–61. https://doi.org/10.1111/j.1752-1688.2007.00137.x.